Universitat de Girona

EXPERIMENTAL AND ANALYTICAL STUDY OF DELAMINATION CAUSED BY FREE-EDGES AND MATRIX CRACKS IN LAMINATED COMPOSITES

Lierni Zubillaga Eceiza

Dipòsit legal: Gi. 2040-2014
http://hdl.handle.net/10803/284759

DOCTORAL THESIS

Experimental and analytical study of delamination caused by free-edges and matrix cracks in laminated composites

Lierni Zubillaga Eceiza

2014

Universitat de Girona

DOCTORAL THESIS

Experimental and analytical study of delamination caused by free-edges and matrix cracks in laminated composites

Lierni Zubillaga Eceiza

2014

DOCTORAL PROGRAM IN TECHNOLOGY

Supervised by: Albert Turon

A thesis submitted for the degree of Doctor of Philosophy by the

University of Girona

To whom it might concern,

Dr. Albert Turon Travesa, Professor at the University of Girona of the Department of Enginyeria Mecànica i de la Construcció Industrial,

CERTIFY that the study entitled *Experimental and analytical study of delamination caused by free-edges and matrix cracks in laminated composites* has been carried out under his supervision by Lierni Zubillaga Eceiza to apply the doctoral degree with the International Mention.

Girona, May 2014

Dr. Albert TuronTravesa

Universitat de Girona, Spain

Bizitzaren bidean bidailagun asko izaten ditugu,

denak omen dute guregan eragina

baina batzuek besteek baino arrasto hangiago uzten dute.

ZUENTZAT: Orain arte egon zaretenontzat eta oraindik jarraitzen duzuenontzat.

Mila esker.

Aknowledgements

Firstly, I will like to thank my supervisor Dr. Albert Turon for giving me the opportunity to carry out my thesis under his supervision. I really appreciate the patience you had with me during the guidance of this work and all the contribution you made.

I would like to acknowledge the Deparment of Mechanical Engineering and Industrial Construction of the University of Girona, and particularly to the research group Analysis of Advanced Materials for Structural Design (AMADE) for the collaboration with IK4-Ikerlan to achieve my thesis.

I will like to express my gratitude to IK4-Ikerlan and especially to Jokin Mujika and Xabier Sagartzazu to give me the chance and offer me the scholarship to develop the work of this thesis.

I also wish to thank Peter Linde and Stephane Madhi from Airbus for the partial funding of this research work. Further for the review and comments you did during the development of iCOMP project.

I would also like to acknowledge Dr. Nicolas Carrere for giving me the opportunity to do a research stay at ENSTA Bretagne University in Brest (France). Furthermore to the knowledge he shared with me and to Dr. Claudiu Badulescu and Dr. Malick Diakhate for the help when performing the experiments. Many thanks also to the colleagues I met there during my research stay.

Tesi hau egin dudan bitartean IK4-Ikerlanen izan ditudan lankide eta lagunak eskertu nahiko nituzke. Nahiz eta zuekin nahi beste denbora egoteko aukerarik ez dudan izan, bueltatzean etxean moduan sentiarazi nauzuelako. Baita ere zuen laguntza eta animoak eman dizkidazuelako. Mila esker. Joseba, Iñigo, Mikel A., Mikel C, Aitor, Iban D, Iban R, Eusebio, Javi, Gorka, Abel, Aitziber, Asier, Idurre, Ane, Jon, Ander, Adrian, Nagore, Sole,... Horrezgain nirekin tesi honen jarraipen zuzenagoa egin duzuenoi, Iker, Adrian, Andoni... eta beste guztioi baita ere.

M'agradaria donar les gracies a la gent que s'ha involucrat directament en aquesta tesis: A en a Josep Costa per les seves contribucions i comentaris. En el aspecte teòric a en Pere Maimí i en el aspecte experimental a en Jordi Renart. També a la gent que m'ha ajudat directament: Carlos Sarrado i Gerard Guillamet, i als tècnics del laboratori, Yunior Batista i Javi Bonilla. I pels moments bons que he compartit amb tots els que feu AMADE: Marc, Marta, Cristina M., Pere, Magda, Lorena, Emili, Dani, Tiina, Joan Andreu, Tamer, Edu O., Edu M., Irene, Natina, Rina... Moltes gràcies.

Tesi hau egiterako orduan, atzera eta aurrera ibiltzean Euskal Herrian utzi izan ditudan lagun guztiei eskerra. Baita bueltatzen nintzen aldi bakoitzean esku zabalik hartzeko prest egon zaretelako. Batez ere beti hor egon zaretelako: Denis, Izaro, Maddi, Iratxe, Haizea,... Eskerrik asko.

Porque esta tesis también ha hecho su aportación en el ámbito personal, a la gente nueva que ha traído a mi vida. Sobre todo a Xevi y Aridna. Gracias .

Azkenik etxekoei aitari eta amari, hartu izan ditudan erabakietan beti lagundu nautelako eta zuei esker izan ez balitz ez nintzatekeelako honaino iritsi izango. Baita gutxi ulertu arren beti arreta eta galdezka ibili diren amona eta amamari ere. Eskerrik asko bihotz-bihotzez.

List of figures

List of tables

List of symbols

Symbol	Description	Unit
L	Laminate length	mm
w	Laminate width	mm
N	Laminate load per width	N/mm
M	Laminate load per width	N/mm
A	Classical Laminate Theory in-plane stiffness matrix	N/mm
B	Classical Laminate Theory coupling matrix	N
D	Classical Laminate Theory bending matrix	Nmm
U	Elastic energy stored in a laminate	J
s	Delamination length	mm
l	Transition zone length	mm
m	Outer or inner ply	
G	Energy release rate for the extension of an interlaminar crack	kJ/m^2
G_c	Fracture toughness of the interface	kJ/m^2
E_{11}	Young modulus in fiber direction	MPa
E_{22}	Young modulus in fiber perpendicular direction (in-plane)	MPa
υ_{12}	Poisson's Coefficient	
G_{12}	Shear modulus	MPa
S	Compliance matrix	m^2/N
σ_{ply}	Ply stresses	MPa

σ_{11}	Stress in fiber direction in local axis	MPa
σ_{22}	Stress in transversal direction in local axis	MPa
σ_{12}	Shear Stress in local axis	MPa
$X^{MD}{}_{i}$,$X^{MD}{}_{ij}$	Strength parameters used in the MCID failure criterion	MPa
Y^{T}	Transverse strength	GPa
G_{Ic}	Mode I Fracture Toughness	kJ/m^2
G_{IIc}	Mode II Fracture Toughness	kJ/m^2
k	Geometric parameter	
t	Ply thickness	mm
ε_{xx}	Applied strain in global axis	
d_1	Crack length	mm
$G(x)$	Available energy	kJ/m^2
$\bar{A}(x)$	Dimensionless parameter	
E_{xx}	Equivalent Young modulus	MPa
d_2	Distance from the corner	mm
σ_c	Material strength	MPa
k_{13}	Dimensionless parameter	
d^*	Nucleation length	mm
L_c	Characteristic fracture length	mm
h	Laminate thickness	mm
ε_c	Initiation strain	
τ	Tractions	MPa
Δ	Displacement jumps	mm
τ_0	Damage initiation threshold	MPa

d	Damage variable	
Δ^f	"Damage minimum displacement jump"	Mm
u_i	Displacement in direction i	mm
x	Position	mm
θ	angle	^{o}
ψ^ρ	Free energy per unit surface	J/mm^2
δ_{ij}	Kroenecker delta	
K	Penalty stiffness	N/mm^3
λ	Norm of displacement	mm
r	Damage threshold	

List of acronyms

Acronym	Description
CFRP	Carbon Fiber Reinforced Polymer
CLT	Classical Laminate Theory
C.V/COV	Coefficient of Variation
CZE	Cohesive Zone Element
CZM	Cohesive Zone Model
DIC	Digital Image Correlation
FE	Finite Element
FEM	Finite Element Model/Method
FF	Fiber Failure
FFM	Finite Fracture Mechanics
INTA	Instituto Nacional de Técnica Aeroespacial
LaRC	Langley Research Center
MDIC	Matrix Crack Induced Delamination
QI	Quasi-isotropic
TC	Transverse Cracking
x-FEM	Extended-Finite Element Method

List of publications

This Ph.D. thesis has been prepared as a compendium of papers, according to the regulations of the University of Girona (Normativa d'ordenació dels ensenyaments universitaris de doctorat de la Universitat de Girona Aprovada pell Consell de Govern en la sessió 3/12, d'abril de 2012). The thesis includes three original papers: one paper that has already been published in a peer-reviewed journal; and two others that have already been submitted, which are under revision at the moment of preparing this document.

The complete references of the papers comprised in this thesis, the impact factors, quartile, and category of the journals are:

- L. Zubillaga, A. Turon, P. Maimí, J. Costa, S. Mahdi, P. Linde. An energy based failure criterion for matrix crack induced delamination in laminated composite structures. Composite Structures 2014;

doi:http://dx.doi.org/http://dx.doi.org/10.1016/j.compstruct.2014.02.015

(Impact Factor: 2.23 , Journal 4 of 24, *Quartile 1*, Category: *Material Science, Composites*)

- L. Zubillaga, A. Turon, J. Renart, J. Costa, P. Linde. An experimental study on matrix crack induced delamination in composite laminates. Submitted to Composite Structures.

(Impact Factor: 2.23 , Journal 4 of 24, *Quartile 1*, Category: *Material Science, Composites*)

- L. Zubillaga, N. Carrere, A. Turon, G. Guillamet, P. Linde. Experimental and numerical analysis of free-edge delamination by means of a two-fold criterion and a cohesive zone model. Submitted to Composite Part A: Applied Science and Manufacturing.

(Impact Factor: 2.74 , Journal 2 of 24, *Quartile 1*, Category: *Material Science, Composites*)

The three papers have been published in (or submitted to) journals with impact factors within the first quartile, according to the 2013 Journal Citation Reports.

Table of contents

Summary

In the last decades, the use of laminated composites, such as Carbon Fiber Reinforce Polymer (CFRP), has increased in many industrial sectors. Many research have been done, from the development of new manufacturing technologies to the study of the material failure modes. In the scope of failure mechanisms different damage mechanism can appear in laminated composites. Therefore, new failure criteria and constitutive models are needed to describe properly the mechanical response of the composite parts up to failure.

Among the different damage mechanisms, delamination or interlaminar failure is one that concerns structural designers. Delamination reduces the load-carrying capacity of composite structures and may compromise structural integrity. Because of that, an effort has been done by the scientific community to promote the development of analysis models to anticipate the onset and propagation of delamination. However, there is a lack of suitable models to predict delamination to be used during the initial design stages of the structural components.

In this work, two different sources of delamination have been studied both experimentally and analytically: free-edge induced delamination and matrix crack induced delamination.

In matrix crack induced delamination scope, a new failure criterion has been proposed. The failure criterion has been validated with experimental data available in the literature and with the results obtained with a dedicated test campaign. The tests were designed to monitor the damage evolution of the specimens when loaded in tension.

In regards to the free edge delamination, two approaches have been analysed to determine delamination onset due to free-edges effects: the coupled criterion and the cohesive zone elements. In order to compare both models, an experimental campaign to study free-edge delamination has been done. A good agreement between the predictions of the two different approaches and the experimental data has been obtained. The

suitability of the models for the prediction of the delamination onset depends on the complexity of the studied structure.

Resumen

En los últimos años se ha incrementado el uso de materiales compuesto en aplicaciones tecnológicas avanzadas. Esto se debe a los avances científicos y tecnológicos que se han realizado empezando desde la fabricación hasta el conocimiento del comportamiento mecánico de los mismos. Este tipo de materiales presentan varios tipos de fallo, es por ello que se necesitan modelos constitutivos y criterio de fallos específicos para los materiales compuestos. Estos modelos y criterios deben tener la capacidad de predecir el proceso de daño que sufren hasta su rotura.

Entre los diferentes mecanismo de daño que se producen en los compuestos la deslaminación o el fallo interlaminar es uno de los que más preocupa a los diseñadores estructurales. La deslaminación puede reducir la capacidad de carga de los compuestos y puede comprometer la integridad estructural. En la actualidad existen varios modelos capaces de predecir correctamente tanto la iniciación como la propagación de la deslaminación, pero estos tiene un coste computacional muy elevado y no son adecuados para emplearlos en el predimensionamiento de la estructuras.

Es en este contexto donde se desarrolla esta tésis, en la que se desean proponer métodos que permitan predecir la deslaminación en las primeras etapas del diseño estructural. En este trabajo se han estudiado, tanto experimentalmente como analíticamente, dos distintos tipos de deslaminación: la deslaminación por efecto de borde y la deslaminación provocada por las grietas de la matriz .

En cuanto a la deslaminación provocada por las grietas de la matriz se ha planteado un nuevo criterio de fallo que se evalúa a partir de las tensiones locales de cada lamina del laminado. Este criterio se ha validado con datos experimentales encontrados en la bibliografía. Paralelamente se ha realizado una campaña experimental para la evolución del daño al cargar las probetas a tracción. Se ha comprobado que el criterio desarrollado permite predecir lo que se observa experimentalmente.

En consideración a la deslaminación por efecto de borde, se han analizado dos modelos: el criterio acoplado y una metodología de análisis basada en elementos

cohesivos. Se llevado a cabo una segunda campaña experimental con la finalidad de observar el fallo por la deslaminación iniciada por un grieta generada en el borde de la probeta. Se ha obtenido una buena predicción mediante los modelos de los fallos producidos, concluyendo que la idoneidad del cada modelo depende de la complejidad de la estructura a diseñar.

Resum

Durant els últims anys, s'ha produït un increment important en l'ús de materials compòsits en aplicacions d'altes prestacions tecnològiques. Aquest increment es deu principalment al avenços científics i tecnològics que s'han realitzat tant pel que fa a als sistemes de producció com a la comprensió dels diferents mecanismes de dany que experimenten aquests materials. Contràriament al que succeeix en els metalls, es habitual que es desenvolupin diferents mecanismes de dany en una estructura de material compòsits. Aquests mecanismes de dany, bé sigui per si mateixos, bé sigui per la interacció entre ells, poden provocar el col·lapse de l'estructura. És per tant imprescindible una bona comprensió d'aquests mecanismes de dany així com disposar de mètodes d'anàlisi, basats en criteris de falla i/o models constitutius, que permetin anticipar la falla en compòsits. És també d'una de gran rellevància que aquest mètodes d'anàlisi es puguin incorporar des de les primeres etapes del disseny de nous elements.

Entre els diferents mecanismes de falla que existeixen, la delaminació o falla interlaminar és un dels mecanismes que més preocupa als dissenyadors estructurals. L'aparició de delaminacions en l'estructura pot reduir considerablement la capacitat de càrrega d'aquesta podent arribar a comprometre'n la integritat estructural. Tot i que existeixen diferents models per predir la iniciació i/o propagació de la delaminació, el cost computacional d'aquests fan que no es puguin incorporar a les etapes de disseny de nous elements estructural.

És en aquest camp, el del desenvolupament de mètodes que permetin anticipar la delaminació des de les primeres etapes del disseny estructural, en el que es desenvolupa aquesta tesis. Més concretament, s'han estudiat tant d'un punt de vista experimental com analític dos tipus diferents de delaminació: delaminació produïda per efectes de vora als extrems lliures del laminat i la delaminació produïda per les esquerdes que es troben a la matriu.

Pel que fa a la delaminació originada per esquerdes en la matriu, s'ha desenvolupat un nou criteri de falla que s'avalua a partir de les tensions locals a les diferents capes del

laminat. Aquest criteri ha estat validat amb dades experimentals de la bibliografia. Paral·lelament s'ha dissenyat una campanya d'assajos per tal analitzar la evolució del dany quan diferents laminats es carreguen a tracció. S'ha comprovat que el criteri de falla desenvolupat permet explicar el que s'observa en els experiments.

Pel que fa a la predicció de la delaminació per efectes de vora, s'han analitzat dos models diferents: un criteri acoblat i una metodologia d'anàlisi basada en elements cohesius. A fi de comparar les prediccions dels dos models, s'ha fet una segona campanya experimental en provetes dissenyades perquè fallin degut a la propagació d'una esquerda provocada per efectes de vora. S'ha obtingut una bona predicció de les càrregues de falla amb dos models, concloent que cada model es millor dependent de la complexitat de la estructura.

1 Introduction and Objectives

1.1 Introduction

Lightweight structures made of polymer-based composite materials are nowadays used in a wide range of technological applications. The outstanding specific stiffness and strength of fiber reinforced polymers (FRP) in combination with better corrosion and fatigue resistance has allowed the increase of composite materials in aircraft and aerospace structures. Moreover, the properties of composites can be tailored to particular applications and capabilities for sensing, changing shape or self-healing can also be included. Their use is rising exponentially replacing traditional materials. As an example, the amount of composite materials used on an Airbus A380, is up to 25% of its weight, while in the newest Boeing 787 and Airbus A350 over the 50% of its structural weight corresponds to composite materials. Moreover, in the last decades, the use of such materials has spread to other fields i.e. the naval and wind-turbine industry, F1 competition and yacht racing.

Unlike metals, when analyzing the composite structures made of CFRP many different failure mechanisms should be considered. Some of them (matrix cracking longitudinally or transversally, fiber kinking, fiber breakage) occur within the lamina and some others in the interface between to neighboring laminas (delamination).

Historically, the first applications where CFRP were used the theories/criteria of metallic design were adapted to be apply with composites. As a consequence, for many years, mainly the quasi-isotropic configuration, also known as "Black Aluminum", were used. However, this approach does not exploit the mechanical properties of polymer-based composite materials. To move away from this approach, a deep understanding of the different damage and failure mechanisms that may develop in laminated composites was needed. Many years of research in the material behavior has lead to a better understanding of the failure mechanisms and different failure criteria have been proposed for the design of laminated composites. As a consequence, from the first applied maximum strain criterion to more complex failure criteria taking into account the different types of damage and/or incorporating geometrical parameters (like lamina thickness) have been developed.

Most of the failure criteria available are focused on intralaminar damage. However, the interlaminar stresses that appear at the interface between adjacent plies together with the poor interface properties of conventional laminates lead interlaminar failure to drive most of the composite structures design. The severe consequences of delamination on the load-carrying capacity of laminated composite structures have prompted the scientific community to endeavor a systematic effort to develop enhanced analysis models. The aim of the models is to predict the delamination onset and the consequences of the failure development in the integrity of composite structure. Although there exist some analysis models for delamination, their suitability to be incorporated early in the product development process is not straightforward due to the high computational costs involved.

It is in this scope, the development of quick analysis methods for delamination, where the present PhD thesis research has been defined. Quick methods that will be based on post-processing routines able to identify the critical areas of a structural component more prone to delaminate. From the strain and stress fields calculated in a FEM simulation using shell elements, these routines will deliver a failure index at each element indicating whether or not a delamination is likely to occur.

1.2 Objectives

The overall objective of this thesis is to provide quick analysis methods to anticipate delamination in carbon-epoxy preimpregnated composite material structures.

Among the different sources of delamination, two of them, matrix crack induced delamination (MCID) and free-edge delamination, have been studied both theoretically and experimentally. The main objective of the thesis is to provide analysis methods to anticipate delamination in CFRP structures at early design steps and optimize the performance of the laminates. Although the requirement of the quick analysis methods are being easy and fast to apply, they should also be “physically based” and rely on the mechanisms involved in the development of delamination when formulating the analysis method.

In addition, in order to contrast the predictions of the criteria, experimental data is required. The experimental data available in the literature was not sufficient to validate and evaluate the suitability of the analysis methods formulated in this thesis. Therefore, two different experimental campaigns were performed. One specifically dedicated to matrix crack induced delamination and the other one to free-edge delamination.

The specific objectives addressed in this thesis are:

- To obtain a physically based criterion to predict matrix crack induced delamination.

- To carry out an experimental campaign to monitor the damage development during loading a specimen under tensile. The process aimed to observe in the test campaign is the formation of matrix cracks and the onset of delaminations from these cracks.

- To compare the predictions of the proposed criterion for matrix crack induced delamination with the experimental data obtained in the campaign.

- To obtain a methodology for the anticipation of free-edge delamination.

- To carry out an experimental test campaign dedicated to free-edge delamination.

- To compare the experimental data and the analysis methods used to predict free-edge delamination.

- To implement the methods developed as post-processing subroutines.

1.3 Outline of the thesis

The body of this dissertation consists on the three aforementioned manuscripts, which are included in the following chapters.

In chapter 2, a formulation to determine delamination onset from matrix cracks is presented. The model is based on an energy balance between the elastic energy release rate available and the fracture toughness of the material to promote delamination growth. The model considers two different states, the undamaged material and the

damaged one and computes using classical laminate theory the energy release rate available for crack extension. Finally, the predictions obtained with the model are compared to the experimental data available in the literature.

In chapter 3, an experimental campaign is performed to better understand matrix crack induced delamination. Moreover, the failure criterion formulated in Chapter 2 is also used to analyze the experimental observations. Five different lay-ups under tensile loading were tested. The occurrence of the different damage events was visually monitored from pictures of the specimen's edge obtained during the test performance. The comparison of the model with the experimental data has shown the suitability of the failure criterion developed to anticipate the apparition of delamination cracks within the different plies of the laminate.

In chapter 4, free-edge delamination is studied both experimentally and with two different models. A coupled criterion that considers that a stress criteria and an energy condition has to be fulfilled simultaneously to promote delamination and a cohesive element model are compared for the suitability to predict the onset of delamination at free-edges. Additionally, an experimental campaign has been performed to compare the predictions done with both models and the real failure resistance.

The thesis is concluded in Chapter 5 with a summary of the achievements and a discussion of possible avenues for future developments.

The MCID model developed has been implemented as user-written subroutine in the commercial finite element code ABAQUS and MATLAB scripts to generate the required properties to apply the criterion. The details of the subroutine code, some examples of input files and a User Manual are given in the Appendix.

2 An energy based failure criterion for matrix cracking induced delamination in laminated composite structures

L. Zubillaga, A. Turon, P. Maimí, J. Costa, S. Mahdi, P. Linde. An energy based failure criterion for matrix crack induced delamination in laminated composite structures. Composite Structures 2014;

doi:http://dx.doi.org/10.1016/j.compstruct.2014.02.015

Chapter 2 is an exact transcription of this article. It has be rewritten in order to have a consistent format of the entire document.

Abstract

Available failure criteria for the design of laminated composite structures do not explicitly take into account the occurrence of delaminations induced by matrix cracks. However, depending on the material properties, laminate stacking sequence and ply thickness, this failure mode may appear and compromise the structural integrity of the structure. In this work, a failure criterion for predicting matrix cracking induced delamination in laminated composites is presented. The failure criterion is developed within the framework of Fracture Mechanics, by comparing the energy release rate available for delamination extension near a matrix crack and the fracture toughness of the interface. The predicted failure loads agree well with experimental data available in the literature, thus supporting the introduction of this failure criterion into the set of failure criteria usually considered in composite's structural design.

2.1 Introduction

Over recent decades in the field of computational mechanics, a huge effort aimed at reducing time and cost in the design of structural components has been made. It is an enormous challenge for the scientific community to propose models that would enable the simplification of preliminary design steps and the reduction of the size and cost of experimental campaigns required for certification. This is of particular interest when designing composite structures, as distinct failure mechanisms such as matrix cracking, fibre kinking, fibre breakage, and/or delamination have to be taken into account. Within these distinctive failure mechanisms, delamination is a major failure mechanism in composite structures [1]. Reduced fracture toughness and interlaminar strength of laminates may expose the structure to delamination damage and compromise its structural integrity. Delamination could be caused by different sources such as singular stresses at free edges, external impacts or manufacturing defects. An additional delamination cause is related to the presence of matrix cracks, which promote stress concentrations and may induce delaminations at the interface between the cracked ply and the neighbouring ply.

Therefore, even though matrix cracking is not usually treated as a critical failure mode, it may trigger delaminations and promote structural collapse. Experimental evidence of the phenomenon has been reported in the literature [2–6]. Crossman and Wang [2] studied the influence of the centre 90º ply thickness in the observed delamination type and reported that delaminations induced by the presence of matrix cracks were observed for thick plies. Some years later, Johnson and Chang [3,4] analysed the failure mode of specimens with different lay-ups and materials. They observed that matrix cracking induced delamination (MCID) was present in many specimens, especially in those containing higher ply clustering and larger mismatch angles between plies. More recently, Hallett et al. [5,6] studied the effect of the ply clustering in a quasi-isotropic laminate and observed a similar trend: delaminations induced by matrix cracks were visually observed when ply blocking was increased.

In recent years, advanced numerical models have been used to simulate the interaction between matrix cracks and delamination growth. For example, Pettermann et al. [7] combined an intralaminar damage model with interface elements at the neighbouring interfaces to model the interaction in corner angle specimens. Moreover, the latest advances in x-FEM [8,9] are able to model the cracking process of the matrix and the delamination triggered from matrix cracks while avoiding mesh dependence. However, both types of solutions are computationally very expensive, which compromises their usability in early design stages.

Hence, for early design steps, matrix cracking and delamination failure is often accounted for using uncoupled failure criteria, i.e., it is not considered that one failure mode spurs the other. Delamination failure has been extensively studied and various failure criteria based on different approaches are available in the literature. Most of these criteria are stress-based and define the onset of delamination from the comparison of the through-the-thickness tensile stress and interlaminar shear stresses obtained from FEM models and interlaminar strengths obtained from an experimental campaign. A summary of many of these criteria can be found in Orifici [10]. However, stress-based criteria are not applicable to singular regions and/or in the presence of stress concentrations and they do not account for the interaction between matrix cracks and delamination growth. In the particular case of delamination induced by matrix cracking, there is some early work, where criteria based on Fracture Mechanics are formulated [4,11,12]. These approaches consider an initial crack at the interface between two plies which might propagate in a self-similarly way. By comparing the energy release rate available to promote delamination at the interface and its fracture toughness, a criterion for delamination growth can be established. However, published approaches apply to different loading conditions. The model of O'Brien [11] is well suited to predicting matrix cracking induced delamination if the delamination grows in the laminate midplane ply or near the free edges. The model of Maimi et al. [12] is better suited for cross-ply laminates loaded under generalised plane strain conditions. It is worth mentioning that neither of these two approaches consider mixed-mode delamination growth. Finally, the Johnson and Chang model [4] is formulated under general loading conditions and accounts for the progressive degradation of the plies due to matrix

cracking. However, it is not formulated in the form of a failure criterion evaluated at a ply level and its application requires a higher computational cost. Therefore, to the best of these authors' knowledge, there is a current lack of an MCID failure criterion, evaluated at a ply level, applicable to general loading conditions such as other failure criteria like LaRC [13] and Puck's [14].

Following the work of O'Brien [11] and Maimi et al. [12], in this paper we present a new physically-based criterion for matrix cracking induced delamination. The criterion proposed can predict mixed mode II-III delamination growth at the interface between a cracked ply and the neighbouring ply and can be applied to any arbitrary in-plane loading, laminate stacking sequence and ply thicknesses. The criterion proposed is formulated in terms of stresses and strengths (which depend on the elastic constants of the laminate, critical fracture energies, laminate geometry and the location of the ply in the laminate), so they are easily implemented in a computational framework. Indeed, they have been implemented in a UVARM user post processing subroutine for ABAQUS [15]. Finally, the proposed criterion has been validated with experimental data available in the literature.

2.2 Formulation of a matrix cracking induced delamination failure criterion

The failure criterion is obtained by comparing the elastic energy released in a laminate due to the increase of delaminated area (*s* in Figure 2.1) and the fracture toughness of the interface between plies. Assuming a pristine laminate, without any type of crack or internal damage, the elastic energy stored in the laminate under general loading conditions reads:

$$U = \frac{Lw}{2}\begin{bmatrix} N & M \end{bmatrix}\begin{bmatrix} A & B \\ B & D \end{bmatrix}^{-1}\begin{bmatrix} N \\ M \end{bmatrix} \quad (1)$$

where *L* and *w* are the laminate length and width, respectively, *N* and *M* are laminate loads per unit width and *A*, *B*, *D*, are the stiffness matrix of the laminate and obtained using Classical Laminate Theory.

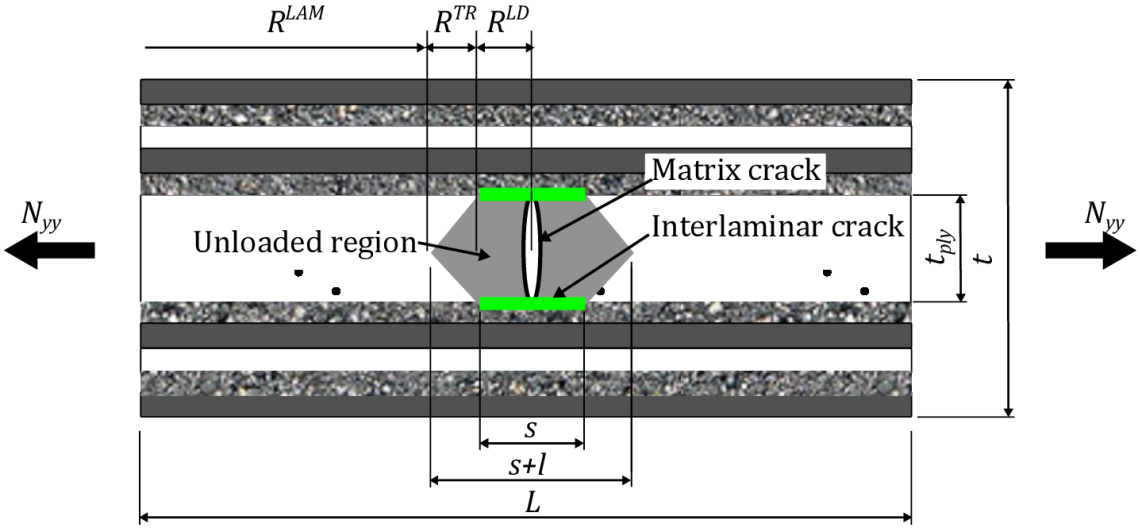

Figure 2.1 Longitudinal section of an uncracked and cracked laminate under tension. The presence of a matrix crack induces a transition region to recover the ply far-field stress.

If a matrix crack appears at a ply, due to the stress recovery region induced near the crack, an amount of elastic energy is released, which creates an unloaded region (grey area shown in Figure 2.1). The elastic energy released, due to the presence of a matrix crack, can be devoted to triggering a new delamination crack at the interface with a neighbouring ply. Three regions with different laminate compliance can be identified: region R^{LAM}, where the laminate compliance is not affected; region R^{LD} where the cracked ply does not contribute to the laminate compliance; and region R^{TR} which is a transition zone where the laminate compliance depends on the shape and length of the stress recovery region. The elastic energy stored in the laminate containing a cracked ply which induces a delamination reads:

$$U = \frac{1}{2}\begin{bmatrix} N & M \end{bmatrix}\begin{bmatrix} A & B \\ B & D \end{bmatrix}^{-1}\begin{bmatrix} N \\ M \end{bmatrix}(L-s-l)w + \frac{1}{2}\begin{bmatrix} N & M \end{bmatrix}\begin{bmatrix} A_{LD} & B_{LD} \\ B_{LD} & D_{LD} \end{bmatrix}^{-1}\begin{bmatrix} N \\ M \end{bmatrix} sw$$

$$+ f^{TR}(N, M, A, B, D)lw \qquad (2)$$

where s is the length of the delamination (region R^{LD}) and l the length of the transition region R^{TR}. It must be pointed out that f^{TR} do not depend on the delamination

length if the distance between consecutive matrix crack is large enough, $\frac{\partial f^{TR}}{\partial s} = 0$ .The energy release rate for the extension of the interlaminar crack *s* is obtained by deriving Equation 2:

$$\mathcal{G} = \frac{1}{2}\frac{\partial U}{wmds} = \frac{1}{2m}\begin{bmatrix} N^T & M^T \end{bmatrix}\begin{bmatrix} \bar{a} & \bar{b} \\ \bar{b} & \bar{d} \end{bmatrix}\begin{bmatrix} N \\ M \end{bmatrix} \quad (3)$$

where:

$$\begin{bmatrix} \bar{a} & \bar{b} \\ \bar{b} & \bar{d} \end{bmatrix} = \begin{bmatrix} A_{LD} & B_{LD} \\ B_{LD} & D_{LD} \end{bmatrix}^{-1} - \begin{bmatrix} A & B \\ B & D \end{bmatrix}^{-1} \quad (4)$$

and $m = 1$ for an outer crack and $m = 2$ for a inner crack. It is also worth noting, that if consecutive matrix cracks are very close, then the estimation of the energy release rate available for delamination extension using Equation (3) becomes a conservative approach, since $\frac{\partial f^{TR}}{\partial s} < 0$.

Various assumptions can be made, depending on the location of the matrix crack within the laminate, to compute the A_{LD}, B_{LD}, D_{LD} terms. This is analysed in greater detail in the following subsection.

Once the energy release rate available for delamination extension is computed, using Equation (3), whether delamination will grow or not can be addressed using the following failure criterion:

$$\frac{\mathcal{G}}{\mathcal{G}_c} = 1 \quad (5)$$

where $\mathcal{G}_c$ is the fracture toughness of the interface when the crack grows under mixed mode II-III loading. As fracture toughness under pure mode III loading is usually not available, it is assumed here that $\mathcal{G}_c = \mathcal{G}_{IIc}$ [16,17].

2.2.1 Determination of the laminate stiffness matrix of the region containing a delamination crack

The laminate stiffness of a region of the laminate containing a delamination induced by a matrix crack, R^{LD} region, can vary depending on their location. Two different situations can be identified, as schematically shown in Figure 2.2:

(a) The matrix crack is located far away from the free edges. It can be assumed that the cross section is under generalised plane strain conditions.

(b) The matrix crack is located close to the free edges (where plane stress conditions apply).

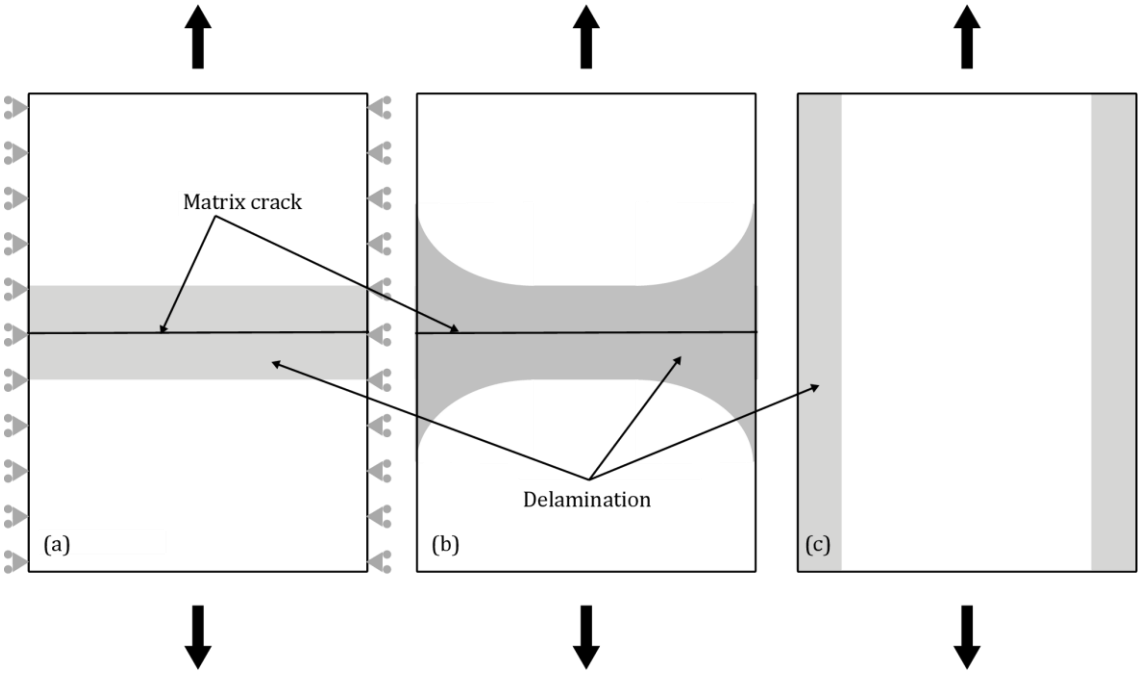

Figure 2.2 Delaminated area in loaded specimens: (a) Matrix crack induced delamination under generalised plane strain conditions. (b) Matrix crack induced delamination near the free edges of the specimen (plane stress). (c) Free-edge delamination due to interlaminar stresses.

Complementary to these two situations, a delamination induced by the interlaminar stresses due to the free-edge effects can also appear (Figure 2.2(c)), but to predict delamination onset an approach similar to the model of O'Brien [11] has to be followed and it is outside the scope of the current paper.

Delamination induced by a matrix crack (Figure 2.2(a) and (b)) can be predicted using Equation (5) with the proper definition of the A_{LD}, B_{LD}, D_{LD} matrices. If the matrix

crack is located far away from the free edge and the transverse stresses are in traction (crack opening), the cracked ply contributes to the laminate stiffness in the fibre direction, but not in the transverse or shear direction. If the transverse stresses are in compression, i.e. closing the transverse crack, then it is assumed that the cracked ply contributes to the laminate stiffness in the fibre and transverse direction, but not in shear.

On the other hand, if the matrix crack is located close to the free edge, the upper and lower sublaminates with respect to the cracked ply become uncoupled and, therefore, the cracked ply is not contributing to the laminate stiffness, except if the orientation of the ply is parallel to the free edge. A summary of the elastic constants considered for the cracked ply is given in Table 2.1. Once the elastic properties of the crack are determined, the A_{LD}, B_{LD}, D_{LD} matrices can be determined using Classical Laminate Theory. Johnson and Chang [4] use a similar approach to compute the stiffness contribution of the cracked ply, but they do not consider crack closure and what would happen if the matrix crack is close and parallel to the free edge.

	E_{11}	E_{22}	υ_{12}	G_{12}
Crack located away from the free edge (generalised plane strain)				
Opening crack ($\sigma_{22} > 0$)	E_{11}	0	0	0
Closing crack ($\sigma_{22} < 0$)	E_{11}	E_{22}	υ_{12}	0
Crack located close to the free edge (plane stress)				
$\theta_{ply}=0^o$	E_{11}	0	0	0
$\theta_{ply}\neq0^o$	0	0	0	0

Table 2.1 Elastic properties of the cracked ply.

2.2.2 Evaluation of the MCID criterion at ply level

The failure criterion for MCID (Equation (5)) can be locally evaluated at a ply level by relating the laminate loads to the local ply stresses. If the laminate is balanced $B = 0$ and under in-plane loading, i.e. $M = 0$, the energy release rate available for crack extension, Equation (3), reads:

$$\mathcal{G} = \frac{1}{2m} N^T \bar{a} N \tag{6}$$

The laminate loads N can be related to ply stresses, $\sigma_{ply}=[\sigma_{11}\ \sigma_{22}\ \sigma_{12}]^T$ using the expression:

$$N = AS\sigma_{ply} \tag{7}$$

where S is the ply compliance matrix. Therefore, Equation (6) can be written as:

$$\mathcal{G} = \frac{1}{2n}\sigma_{ply}^T \chi \sigma_{ply} \tag{8}$$

where

$$\chi = S^T A^T \bar{a} A S \tag{9}$$

Note that S and $\bar{a}$ are evaluated in the local ply coordinate axes and A in the local laminate coordinate axes. It must be noted that if the laminate moments M are relevant or if the laminate is not balanced, then the evaluation of the χ matrix cannot be made with Equation (9). However, in the practical design of laminated structures, the laminates are balanced and if sectional moments are important, reinforcements (stiffeners) are used to provide the rest of the laminate with low sectional moments.

Therefore, using previous equations, the failure criterion for MCID given by Equation (5) can be written as:

$$\left(\frac{\sigma_{11}}{X_1^{MD}}\right)^2 + \left(\frac{\sigma_{22}}{X_2^{MD}}\right)^2 + \left(\frac{\sigma_{12}}{X_6^{MD}}\right)^2 + \frac{\sigma_{11}\sigma_{12}}{X_{16}^{MD}} + \frac{\sigma_{22}\sigma_{12}}{X_{26}^{MD}} + \frac{\sigma_{11}\sigma_{22}}{X_{12}^{MD}} = 1 \tag{10}$$

where

$$X_1^{MD} = \sqrt{\frac{2m\mathcal{G}_c}{\chi_{11}}} \tag{11}$$

$$X_2^{MD} = \sqrt{\frac{2m\mathcal{G}_c}{\chi_{22}}} \tag{12}$$

$$X_6^{MD} = \sqrt{\frac{2m\mathcal{G}_c}{\chi_{66}}} \quad (13)$$

$$X_{12}^{MD} = \frac{2m\mathcal{G}_c}{(\chi_{12}+\chi_{21})} \quad (14)$$

$$X_{16}^{MD} = \frac{2m\mathcal{G}_c}{(\chi_{16}+\chi_{61})} \quad (15)$$

$$X_{26}^{MD} = \frac{2m\mathcal{G}_c}{(\chi_{26}+\chi_{62})} \quad (16)$$

2.2.3 Failure envelope

The failure surface in the plane σ_{22} - σ_{12} for the midplane layer of different quasi-isotropic composites is shown in Figure 2.3. The ply sequence of the laminates analysed is $[90_n/0_n/45_n/-45_n]_{rs}$ where *n* refers to the ply clustering and *r* the number of repetitions. The total number of layers is equal to 32 for all laminates. The material considered in this investigation is T300-934 carbon epoxy from O'Brien [11] with a ply thickness of 0.125 mm. The mechanical properties of the T300-934 carbon epoxy material are given in Table 2.2. It can be observed that the higher the ply clustering, the lower the failure surface for matrix cracking induced delamination (see Figure 2.3).

E_{11}	E_{22}	υ_{12}	G_{12}	Y_T	$\mathcal{G}_{Ic}$	$\mathcal{G}_{IIc}$
134 GPa	10.2 GPa	0.3	5.52 GPa	44.43 MPa	0.216kJ/m^2	0.286kJ/m^2

Table 2.2 T300-934 Mechanical Properties [11]

It is also worth analysing the relevance of the MCID failure criterion in the analysis of laminated composite structures. As matrix cracking is one of the first damage mechanisms to appear in a laminate, it is interesting to analyse whether MCID is the most restrictive failure criterion. To answer this question, the MCID failure criterion and a matrix cracking failure criterion are compared for some specific ply sequences. LaRC criteria [13] for matrix cracking are considered. According to this criterion, the in-situ transverse strength for thin embedded ply is [18,19]:

$$Y_T^{IS} = \sqrt{\frac{4E_{22}\mathcal{G}_{Ic}}{kt\,(1-\upsilon_{12}\upsilon_{21})}} \tag{17}$$

where k is a geometric parameter that depends on the stiffness of the neighbouring layers [20]. If the inner and outer materials have the same Young modulus $k = \pi$. The in situ transverse strength $Y^{IS}{}_T$ is higher than the transverse strength measured in a unidirectional laminate Y_T.

The MCID and the in situ transverse strength for matrix cracking of different quasi-isotropic laminates with the same in-plane stiffness have been computed. The MCID transverse strength obtained for the most external -45^o layer (layer #3 in the laminate stacking sequence) and the most internal -45^o layer (layer #4 $r-1$) are shown in Figure 2.4.

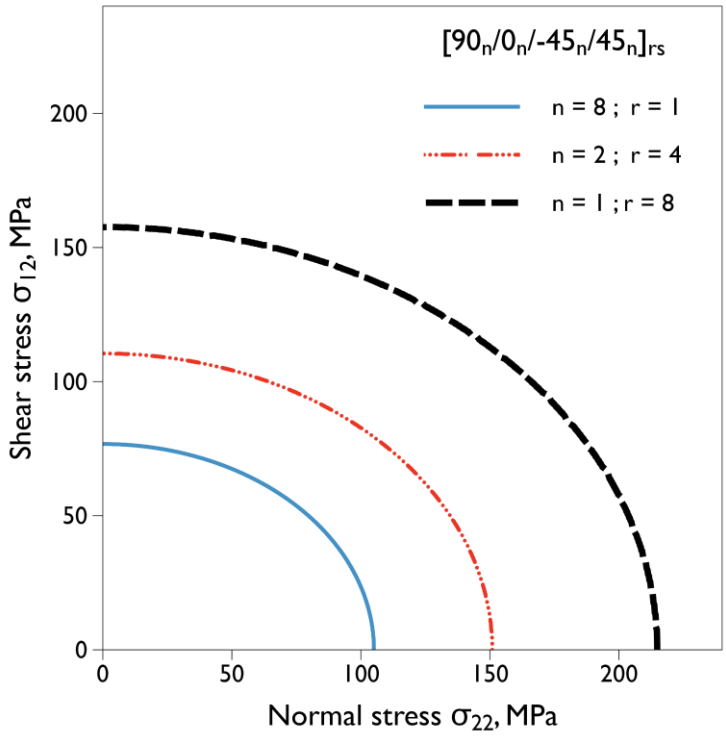

Figure 2.3 MCID failure surface for central 45º ply of T300-934 carbon epoxy quasi-isotropic laminate.

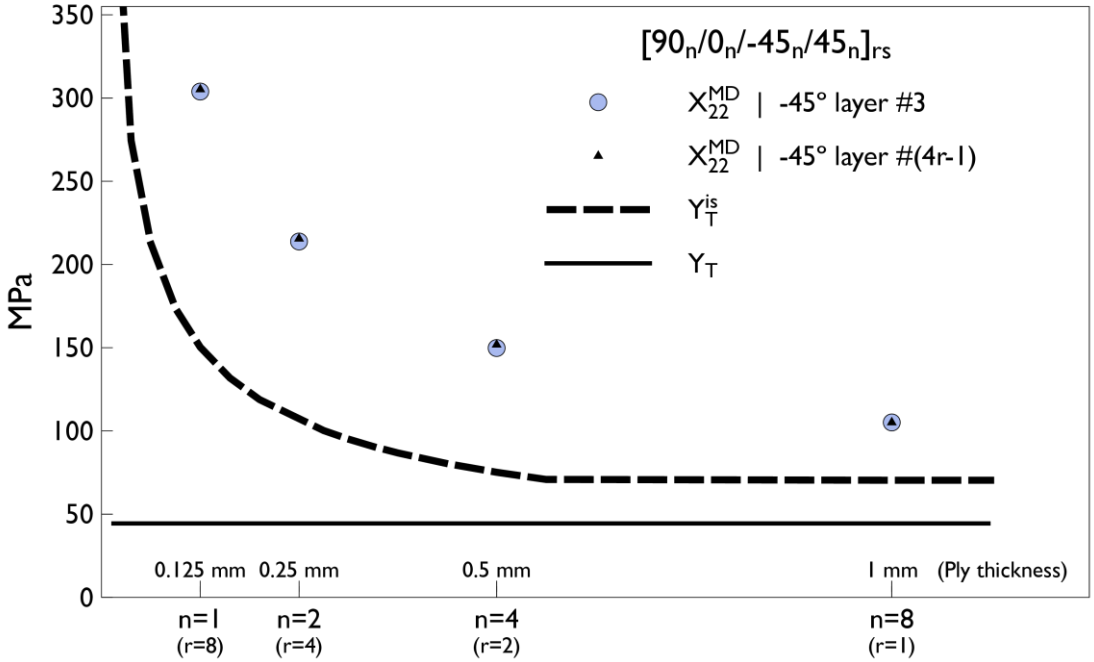

Figure 2.4 Comparison of the transverse strength for matrix cracking and MCID failure of an internal layer in a T300-934 quasi-isotropic laminate.

It can be observed that very similar values are obtained for both layers, although the MCID strength is slightly smaller for the more external layer. The in situ transverse strength for matrix cracking is also plotted in the same figure. The transverse strength for MCID follows a similar trend to the in-plane in situ transverse strength for matrix cracking from the LaRC criteria. The lower the ply clustering, the higher the transverse strength.

Ply	θ	t (mm)	FI_{TC}	FI_{MD}	FI_{FF}
1	90	0.5	0.97	0.71	0.00
2	0	0.5	0.00	0.00	0.33
3	-45	0.5	0.29	0.43	0.12
4	45	0.5	0.29	0.41	0.12
5	90	0.5	0.45	0.27	0.00
6	0	0.5	0.00	0.00	0.33
7	-45	0.5	0.29	0.34	0.12
8	45	1.0	0.3	0.78	0.12

Table 2.3 Failure index of QI laminate $[90_4/0_4/-45_4/45_4]_{2s}$ for an applied laminate strain ε_{xx}=0.5%

The failure index obtained for three failure modes: Fiber Failure (FF), Transverse Cracking (TC) and MCID of the quasi-isotropic laminate with n = 4 are listed in Table

2.3. The FF and TC failure indexes are computed using the LaRC criteria [13]. It can be observed that in the ±45º layers, the failure index for MCID is higher than that of TC. If the failure index for MCID is higher than that of transverse cracking, delamination will grow because of the presence of an existing crack caused by the manufacturing process or previous loading stages or, if there is no preexisting matrix crack, delamination growth will suddenly occur once a matrix crack appears. Therefore, according to the failure indexes obtained, the final failure of this laminate will be driven by delaminations induced by matrix cracks. This is a clear illustration that the MCID transverse strength has to be taken into account in a safe design of a laminate.

2.3 Validation of the failure criteria

The validation of the MCID failure criteria has been performed by comparing the predictions from the proposed formulation with the experimental data from two different independent studies [2,5].

The experimental data obtained by Crossman and Wang [2] has been used to validate the MCID transverse strength. In their study [2], different specimens with laminates $[25/-25/90_n]_s$ with a clustering of the 90º ply ranging between $n = 0.5$ and $n = 8$ were tested under tensile loading.

The different laminates tested in [2] have been simulated using S4 elements in ABAQUS [15]. The MCID failure criterion given by Equation (10) has been implemented as a post-processing tool using the UVARM subroutine available in ABAQUS. The laminate failure strains obtained from the simulations and from the available experimental data are plotted in Figure 2.5. The experimental results showed that, depending on the clustering of the 90º ply, two different failure mechanisms occur: for values of n lower than 3 the failure mode was due to free-edge effects, while for values larger than 3 specimens failed due to MCID. Therefore, the predictions obtained with the numerical models can only be compared with the experimental data for a ply clustering n higher than 3, i.e., for those laminates where MCID was observed in the experimental test. It can be observed that the results obtained using the MCID failure criterion given by Equation (10) and considering the matrix crack located close to the

free edge, are in a good agreement with the experimental data. For values of *n* higher than 3, the difference between the predicted values obtained with the present model and the experimental data is lower than 5%. The difference between these predictions and those obtained with the model formulated by O'Brien [11] are very small.

The failure strain obtained by assuming that there are no matrix cracks close to the free edge is also plotted in Figure 2.5 for comparison. It can be observed that the failure strain obtained in this case is much higher than when considering the matrix crack near the free edge and clearly overestimate specimen failure. It is worth mentioning that, in this case, the results are very close to the predictions obtained by the simplified model presented in Maimi et al. [12]. However, it should be noted that the specimen's failure observed by [2] were due to delaminations that appeared near the free edge and therefore, the predictions of the failure strain considering the matrix crack away from the free-edge cannot be compared with the experimental data. However, it illustrates that free edge cracks are more prone to delaminate. Therefore, it is conservative to assume that the matrix crack is located near the free edge.

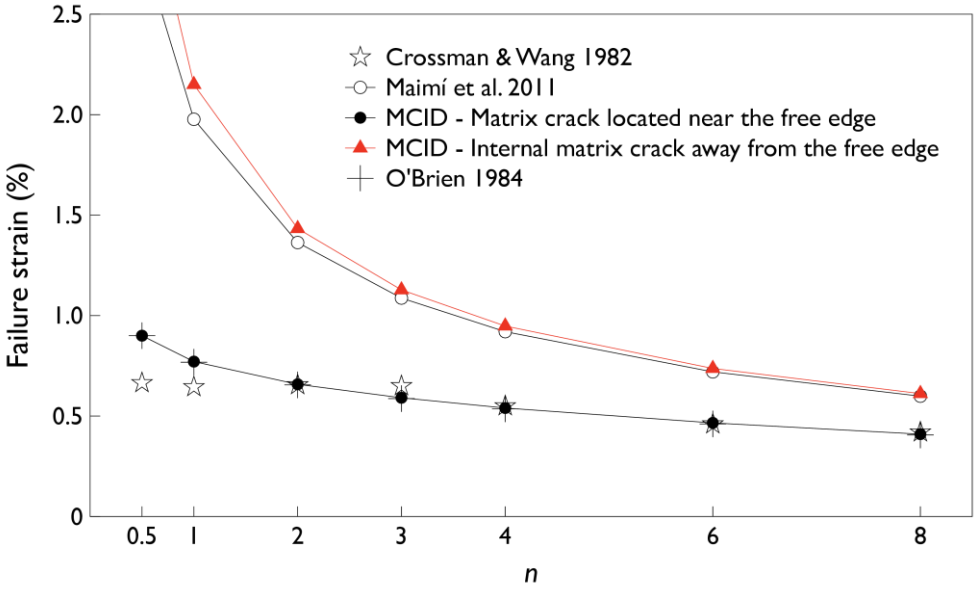

Figure 2.5 Experimental data and numerical predictions of the failure strain of the T300-934 carbon epoxy $[\pm 25/90_n]_s$ laminates tested by Crossman and Wang [2].

The experimental data provided by Crossman and Wang [2] can only be used to validate the model for delamination growth only when transverse tractions are present in the crack plane (90º ply). However, in the experimental campaign of Hallett et al. [5], different quasi-isotropic laminates where tested and delaminations induced by matrix cracks of a 45º ply were observed. Using the model developed in this work, the laminate failure stress due to MCID resulting from the numerical simulations of laminates $[45_n/90_n/-45_n/0_n]_s$ are predicted. The material properties used in the numerical simulations are taken from [21] and summarised in Table 2.4.

E_{11}	$E_{22}=E_{33}$	$G_{12}=G_{13}$	$\upsilon_{12}=\upsilon_{13}$	$\mathcal{G}_{IIc}$
171.0 GPa	9.08 GPa	5.29 GPa	0.32	0.788 kJ/m^2

Table 2.4 Material Properties of IM7/8552 from [21]

The experimental failure stresses for MCID of the interface 45/90 [5] and the numerical predictions using the MCID failure criterion are given in Figure 2.6 and Table 2.5. The MCID failure criterion (Equation (10)), assuming a crack close to the free edge, predicts that the MCID will occur because of the presence of a matrix crack at the outer 45º layer, as observed in the experimental results. The predictions obtained using the MCID failure criterion are in agreement with the experimental data. The influence of the ply clustering is captured by the model and the maximum difference between the numerical prediction and the experimental mean value is lower than 13%, in all cases smaller than the C.V. obtained in the experimental campaign, as shown in Table 2.5.

Lay-up	Width (mm)	Experimental [5] (MPa)	C.V [5] (%)	Numerical Prediction (MPa)	Difference (%)
[45/90/-45/0]s	30	-	-	666	-
$[45_2/90_2/-45_2/0_2]_s$	60	418	13.8	471	12.7
$[45_4/90_4/-45_4/0_4]_s$	120	316	11.4	333	5.4
$[45_8/90_8/-45_8/0_8]_s$	240	222	10.3	235	5.8

Table 2.5 Laminate stress for delamination of 45/90 interface.

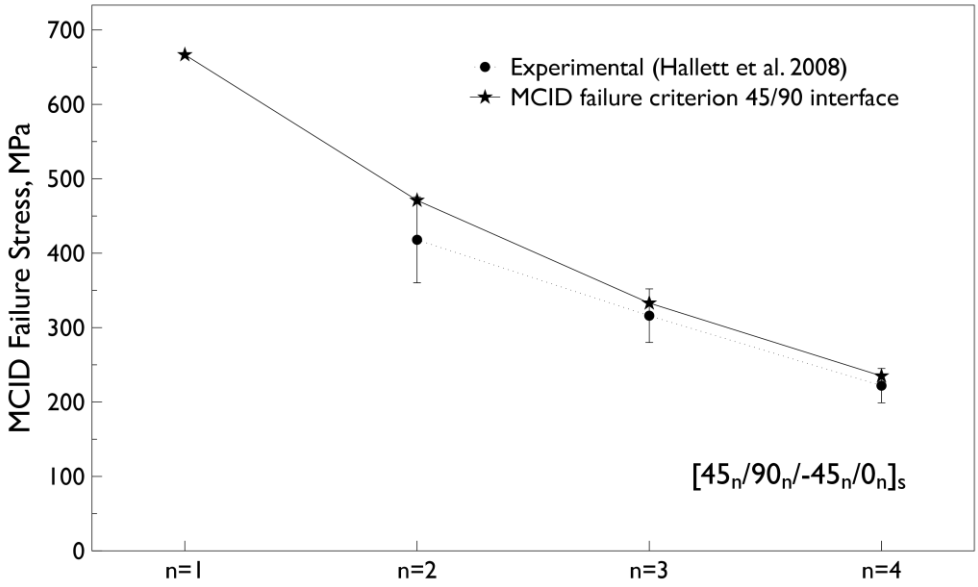

Figure 2.6 Experimental data and numerical predictions of the MCID delamination at the interface (45/90) of quasi-isotropic IM7/8552 carbon epoxy laminates.

2.4 Conclusions

A failure criterion for matrix cracking induced delamination for laminated composites has been presented in this work. The failure criterion has been formulated by comparing the available energy release rate (written in terms of ply stresses), due to the presence of a crack in the matrix and the fracture toughness of the interface. The parameters of the failure criterion are dependent on material properties, ply thickness and laminate compliance properties before and after the presence of a matrix crack.

It has been demonstrated that, for certain laminate configurations, the failure load predicted for MCID is lower than that of fiber failure and matrix cracking. This provides evidence of the convenience of taking MCID into account when designing laminated structures.

The model was implemented in a finite element software as a post-processing tool. Several laminates were simulated and the predicted failure stresses were compared with available experimental data and showed good agreement. Current failure criteria available in the literature do not account for matrix cracking induced delamination, thus,

the failure criterion proposed in this work could be incorporated into a wider set of failure criteria for composites, for instance LaRC or Puck criteria.

Acknowledgments

This work was funded by AIRBUS under the project *iComp - integrated method for the structural design of Composite components*. The authors gratefully acknowledge the support provided by AIRBUS.

The support of the Spanish government through DG-GICYT under contract DPI2012-34465 and MAT2012-37552-C03-03, is acknowledged.

References

[1] Pagano, N.J., Schoeppner, G.A. Delamination of polymer matrix composites: problems and assessment. Comprensive Composite Materials, 2. (ed.) Kelly, A., Zweben, C. Elsevier Science Ltd., Oxford (UK) 2000.

[2] Crossman F.W. and Wang A.S.D. The dependence of transverse cracking and delamination on ply thickness in Graphite/Epoxy laminates. Damage in Composite Materials, ASTM STP 1982; 775:118-139.

[3] Johnson. P and Chang F. Characterization of Matrix Crack Induced Failure- Part I: Experiments. Journal of Composite Materials 2001; 35(22):2009-2035.

[4] Johnson. P and Chang F. Characterization of Matrix Crack Induced Failure- Part II: Analysis and verifications. Journal of Composite Materials 2001; 35(22):2037-2074.

[5] Hallett S.R., Jiang W., Khan B. and Wisnom M.R. Modelling the interaction between matrix cracks and delamination damage in scaled quasi-isotropic specimens. Composite Science and Technology 2008; 68(1):80-89.

[6] Wisnom, M.R., Khan, B. and Hallett, S.R., 2008. Size effects in unnotched tensile strength of unidirectional and quasi-isotropic carbon/epoxy composites. Composite Structures, 84(1), pp. 21-28.

[7] Pettermann H.E., Rama E, Reisinger A and Gager J. Delamination induced ply damage - Nonlinear simulations accounting for degradation of layer and interface properties simultaneously. In: Abstract book IV ECCOMAS Thematic Conference on the Mechanical Response of Composites. Sao Miguel, Azores, Portugal. 25-27 September 2013. p.40.

[8] Iarve E., Gurvich M., Mollenhauer D., Rose C.A and Dávila C.G. Mesh-independent matrix cracking and delamination modeling in laminated composites. International Journal for Numerical Methods in Engineering 2011; 88(8):749-773.

[9] Van Der Meer F.P and Sluys L.J. Continuum models for the analysis of progressive failure in composite laminates. Journal of Composite Materials 2009; 43(20):2131-2156.

[10] Orifici AC, Herszberg I and Thomson RS. Review of methodologies for composite material modelling incorporating failure. Composite Structures 2008; 86(2):194-210.

[11] O'Brien TK. Analysis of local delamnations and their influence on composite laminate behaviour; NASA Technical Memorandum 85728. 1984.

[12] Maimi P, Camanho PP, Mayugo JA, Turon A. Matrix cracking and delamination in laminated composites. Part I: Ply constitutive law, first ply failure and onset of delamination. Mechanics of Materials 2011;43(4):169-185.

[13] Camanho PP, Davila CG, Pinho ST, Iannucci L, Robinson P. Prediction of in situ strengths and matrix cracking in composites under transverse tension and in-plane shear. Composites Part A: applied science and manufacturing 2006; 37(2): 165-176.

[14] Puck, A. and Schurmann, H. 2002, "Failure analysis of FRP laminates by means of physically based phenomenological models", Composites Science and Technology, vol. 62, no. 12-13 SPECIAL ISSUE, pp. 1633-1662.

[15] ABAQUS 6.11 User manual.

[16] Li, J., Sen, J.K., Analysis of frame-to-skin joint pull-off tests and prediction of the delamination failure. *42nd AIAA/ASME/ASCE/AHS/ASC Structures, Structural Dynamics and Materials Conference, Seattle, WA, USA,* 2000.

[17] Li, J., Three-Dimensional effects in the prediction of flange delamination in composite skin-stringer pull-off specimens. *15th Conference of the American Society for Composites Texas, USA*, 2000.

[18] Dvorak GJ and Laws n. Analysis of Progressive Matrix Cracking in Composite Laminates II: First ply failure. Journal of Composite Materials 1987; 21 (4): 309-329.

[19] Maimi P., Gonzalez E., Camanho PP., Comment to the paper 'Analysis of Progressive Matrix Cracking in Composite Laminates II. First Ply Failure' by George J Dvorak and Norman Laws, Journal of Composite Materials 2013; DOI: 10.1177/0021998313483986.

[20] Hutchinson J.Wand Suo Z. Mixed mode cracking in layered materials. Advances in applied mechanics, Volume 29. 1992. Academic Press Inc. San Diego CA. USA.

[21] Camanho, P.P., Maimi, P., and Davila, C.G., "Prediction of Size Effects in Notched Laminates Using Continuum Damage Mechanics," Composites Science and Technology, Vol. 67, No. 13, 2007, pp. 2715-2727.

3 An experimental study on matrix crack induced delamination in composite laminates

L. Zubillaga, A. Turon, J. Renart, J. Costa, P. Linde. An experimental study on matrix crack induced delamination in composite laminates. Submitted to Composite Structures.

Chapter 3 is an exact transcription of this article. It has be rewritten in order to have a consistent format of the entire document.

Abstract

Matrix crack induced delamination is one of the predominant failure mechanisms in laminated composites under off-axis loading. However, there exist a reduced number of experimental studies on the literature specifically devoted to this failure mechanism. In this work, an experimental campaign focused on the occurrence of matrix cracking and delamination induced by matrix crack is presented. Five different carbon-epoxy lay-ups have been tested under tensile load, leading to different damage evolutions. The experimental data has been compared with a failure criterion recently developed by the authors. A good agreement between the experimental data and the predictions of the failure criterion has been obtained.

3.1 Introduction

The increased use of advanced composite laminates in primary structures of commercial aircraft requires a thorough understanding of the inelastic response of composites under general loading conditions. One of the most relevant mechanisms that contribute to the loss of stiffness and to the structural collapse of composite structures is delamination. Due to the presence of matrix cracks, or edge effects, the different plies tend to delaminate preventing the stress transfer between plies.

Although there are many works in the literature focused on the onset and growth of delamination cracks, few of them analyse the onset and growth from matrix cracks. Crossman and Wang [1], in the early 80's, made a dedicated test campaign to analyse, using X-ray radiography, the influence of the ply thickness of the 90º lamina on the damage mechanisms involved in the failure of a $[25/-25/90_n]_s$ laminate. The thickness of the 90º ply was defined by blocking n layers (n= 0.5÷8). Two different failure types were observed: free-edge delamination occurred for the thinner 90º lamina whereas matrix crack induced delamination occurred for the thicker ones. The transition point between both failure types was at about n=3. More recently, Johnson and Chang [2,3] performed a very extensive campaign with different laminates and material systems and analysed the different failure mechanisms involved in failure. Tensile tests were stopped periodically to make X-rays radiographies to the specimens. They also reported the failure load obtained for the different configurations and concluded that the ply thickness and laminate orientation have an important influence on the failure mode.

Hallett et al. [4] also reported delamination onset and growth induced by matrix cracks. In this case the influence of the scaling on the failure mode was studied in a quasi-isotropic or "black-aluminium" lay-up by testing specimens scaled in dimensions and with blocking plies. A similar testing methodology than in [2,3] was conducted. The main conclusion of this work was that large ply blocking decreases the failure load. Moreover, smaller specimens did not present any delamination until final failure, while the rest presented one or two interfaces with delamination at lower strain levels than the ultimate strain.

More recently, Guillamet et al. [5] performed an experimental study of the influence of the ply thickness and the off-axis load on a quasi-isotropic non-crimp fabric laminate. A quasi-isotropic composite panel with two different regions, with or without ply clustering, was manufactured. The specimens were cut from the panel with different orientations in order to apply different off-axis loads. Although all the resulting laminates were quasi-isotropic in regards of the in-plane stiffness, the experimental campaign revealed a high anisotropy in strength, especially when the applied load was not coincident with any of the 0º oriented plies of the laminate. In these cases, delamination induced by matrix cracks (MCID) was the leading cause of the specimen's failure. It was also reported that there is an inverse relationship between the ply thickness and the laminate stress for the apparition of MCID cracks.

On the other hand, there exist several failure criteria available in the literature to predict the occurrence of the different damage mechanisms that can take place in laminated composites [6]. However, a reduced number of works are focused on the prediction of delamination failure induced by the presence of matrix cracks. In a recent paper [7], the authors proposed a new failure criterion based on previous works of O'Brien [8] and Maimí et al. [9]. In addition, there are computational methodologies to predict delamination induced by matrix cracking, such as using cohesive elements to model intraply and interlaminar damage [10], progressive damage models [11] or the extended finite element method [12]. However, the high computational resources required for these approaches make them suitable only for a detailed progressive damage analysis of composites parts, at the final steps of design, but it is difficult to incorporate them in the early stages of sizing the part.

In this work, an experimental campaign is performed to better understand matrix crack induced delamination. Its objective is to analyze delamination induced by matrix cracks, i.e., to observe the creation of transversal cracks in the matrix and then delamination onset from the crack tips.. The occurrence of the different damage events were monitored by optical inspection of the specimen's edge during the tests. The experimental details are given in Section 3.2 and the results in section 3.3. In Section 3.4, the matrix crack induced delamination (MCID) failure criterion developed by the

authors in a recent work [7] together with the LaRC [13] failure criteria for matrix cracking are used to analyze and discuss the experimental observations. The comparison of the model with the experimental data has shown the suitability of the failure criterion developed to anticipate the apparition of delamination cracks within the different plies of the laminate.

3.2 Materials and Methods

3.2.1 Materials

Five different lay-ups were tested under tensile loading while monitoring the occurrence of the different damage mechanisms.

The specimens were made of unidirectional pre-impregnated carbon-epoxy T800-M21 from Hexcel. They were manufactured in autoclave at Instituto Nacional de Técnica Aeroespacial (INTA) according to standard aeronautic procedures. Their dimensions were 225 mm long and 25 mm wide, the thickness was variable and depended on the layup sequence. Fine graded sandpaper was used to polish the edges of the specimen to be able to observe the different plies and interfaces where delamination might grow.

3.2.2 Test set-up

Tensile tests were performed with a universal servo-hydraulic testing machine 810 MTS. The force was measured with a load cell of 250kN. The tests were conducted under displacement control and the cross head displacement rate was set to 0.15mm/min in order to properly monitor the damage occurrence at the specimen edge. Additionally, an MTS extensometer with a gage length of 25 mm was used to measure the strain of the specimen in the loading direction. Finally, to observe matrix cracking and delamination onset at the coupon edge, a similar methodology to the one used by [14] has been used, where a digital reflex camera Canon EOS550D with a 100mm macro lens was used. The distance between the specimen and the camera support was set between 300mm and 320mm. Pictures of about 50 mm of the specimen length were

taken every 5 seconds and a user-defined software was used to synchronize the pictures taken with the camera and the strains measured with the extensometer.

3.2.3 Test matrix

The specimen definition was done based on the previous work by Johnson and Chang [3], where matrix crack induced delamination was observed for the first three lay-ups of table 3.1. Delamination induced by the presence of a matrix crack is prone to grow at the $\theta/-\theta$ interface of these specimens. In addition, two additional lay-ups were devised based on the predictions of the MCID criterion [7]. These two lay-ups are symmetrical and balanced like the ones proposed by Johnson and Chang [3]. However, for these two cases more than two ply orientations were proposed for each configuration, increasing the number of potential interfaces for delamination onset. Five specimens of each configuration were tested.

Stacking sequence	Specimen Series
$[45_3/-45_3]_s$	MCID-45-c3
$[60_3/-60_3]_s$	MCID-60-c3
$[60_4/-60_4]_s$	MCID-60-c4
$[45_2/-45_2/-60_4/45_2/-45_2/60_4]_s$	MCID-60/45
$[45_2/-45_2/90_4/45_2/-45_2/90_4]_s$	MCID-90/45

Table 3.1 Experimental test matrix

3.3 Results

3.3.1 Stiffness and strength

The results of the stress-strain response for all the layups are shown in figures 3.1 to 3.3. The results of all the specimens of the batch are shown for each stacking sequence, except for the configurations MCID-60-c4 and MCID-60/45. In these configurations only 4 valid results could be obtained due to problems with the data acquisition system.

The stress-strain curves presented a monotonic behavior up to a point where a noticeable change on the laminate stiffness was observed. This point was related to the initiation of different damage mechanisms as shown in section 3.3.2. After this point, two different behaviors were observed: some laminates failed suddenly, while others presented a plateau region with damage accumulation before final failure.

In the case of MCID-45-c3 specimens, three of the specimens (MCID-45-c3-01, 02, 03) presented a very large plateau region, while the other two (MCID-45-c3-04, 05) abruptly failed without developing of a plateau region, as shown in Figure 3.1.

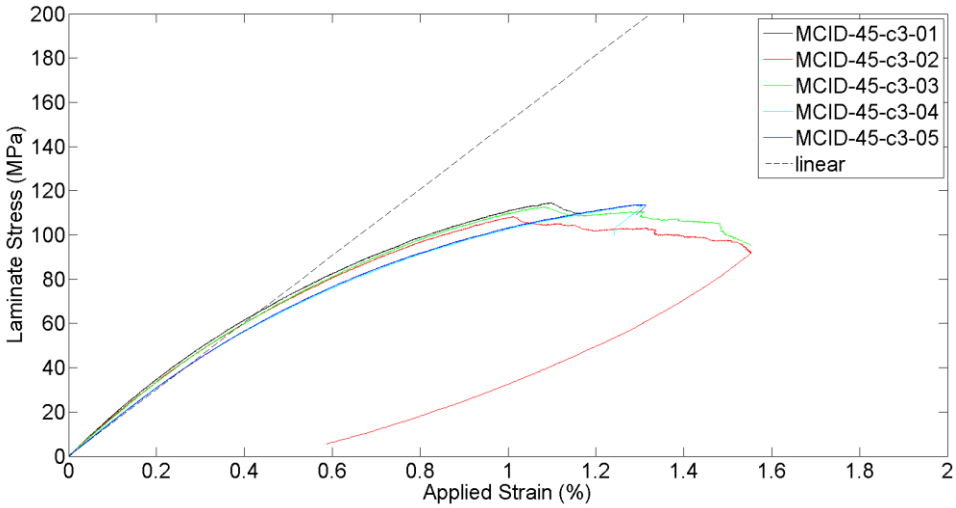

Figure 3.1 Stress-strain curves obtained for $[45_3/-45_3]_s$(MCID-45-c3) lay-up.

The highest scatter in the failure strength was obtained for the $[60_n/-60_n]_s$ laminates (see Figure 3.2). In MCID-60-c3 specimens the stress-strain curves were coincident before failure. However, when analyzing final failure a COV of 10% was found. A similar trend was observed in MCID-60-c4 batch. In this case the COV was of about 16% , which is higher than the one for MCID-60-c3.

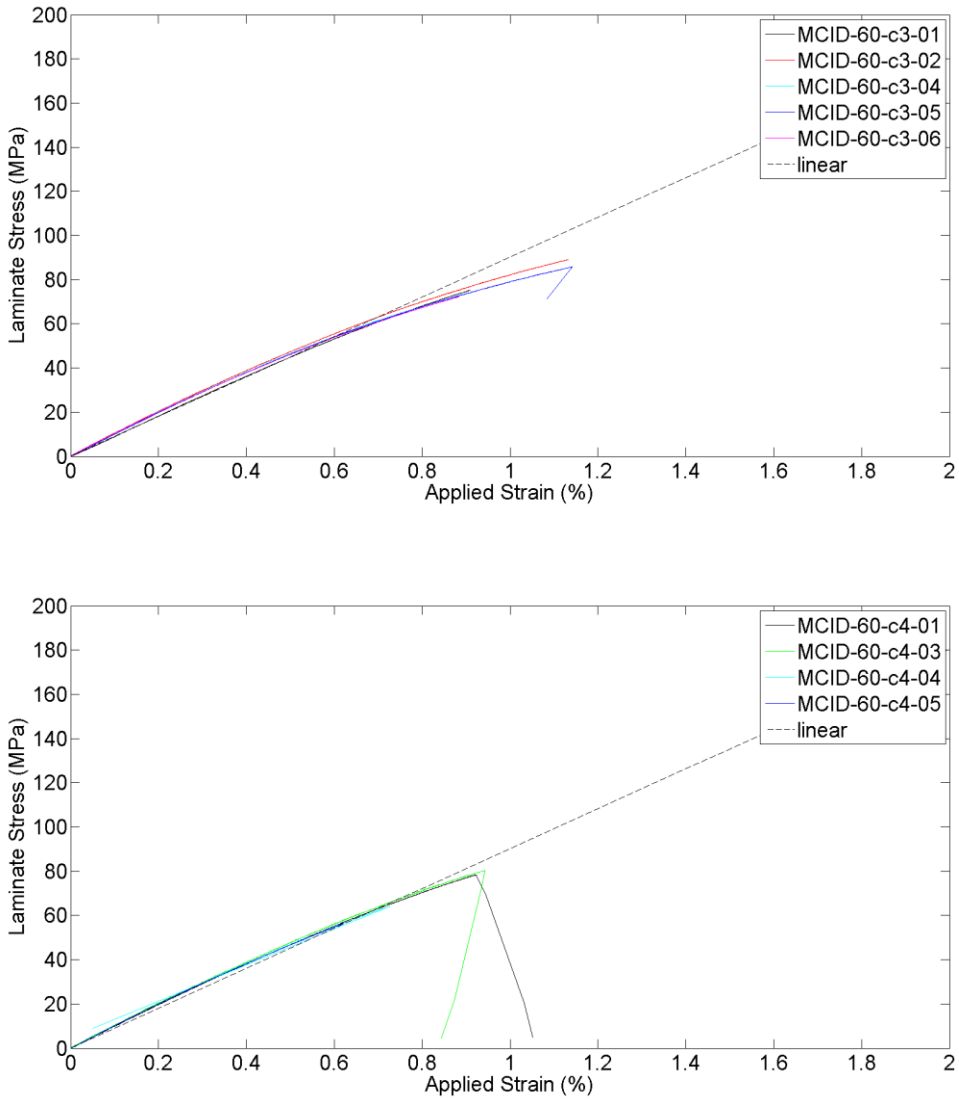

Figure 3.2 Stress-strain curves obtained for $[60_3/-60_3]_s$(MCID-60-c3) and $[60_4/-60_4]_s$(MCID-60-c4) layups.

Figure 3.3 shows the stress-strain curves of the laminates with more interfaces prone to fail (with the stacking sequence $[45_2/-45_2/-\theta_4/45_2/-45_2/\theta_4]_s$ with θ equal to 60º, MCID-60/45, and 90º, MCID-90/45). In MCID-60/45 configuration a monotonic behavior was obtained until a stress around 133 MPa where an important decrease on the laminate stiffness was observed. A "plateau" region followed this point, where loading capacity of the specimens did not increase but a considerable elongation was attained. The plateau region started at a strain of around 1.0% while the final failure was at around 1.8%.

For MCID-90/45 configuration a similar behavior to MCID-60/45 was observed, with a plateau region, at around 130 MPa. However, contrarily to the MCID-60/45 laminate, the plateau region was followed by a stiffness increase and the specimens failed at around 160 MPa. The plateau region appeared for a laminate strain between 0.6%-0.7% and the final failure occurred between 1.3% and 1.6%.

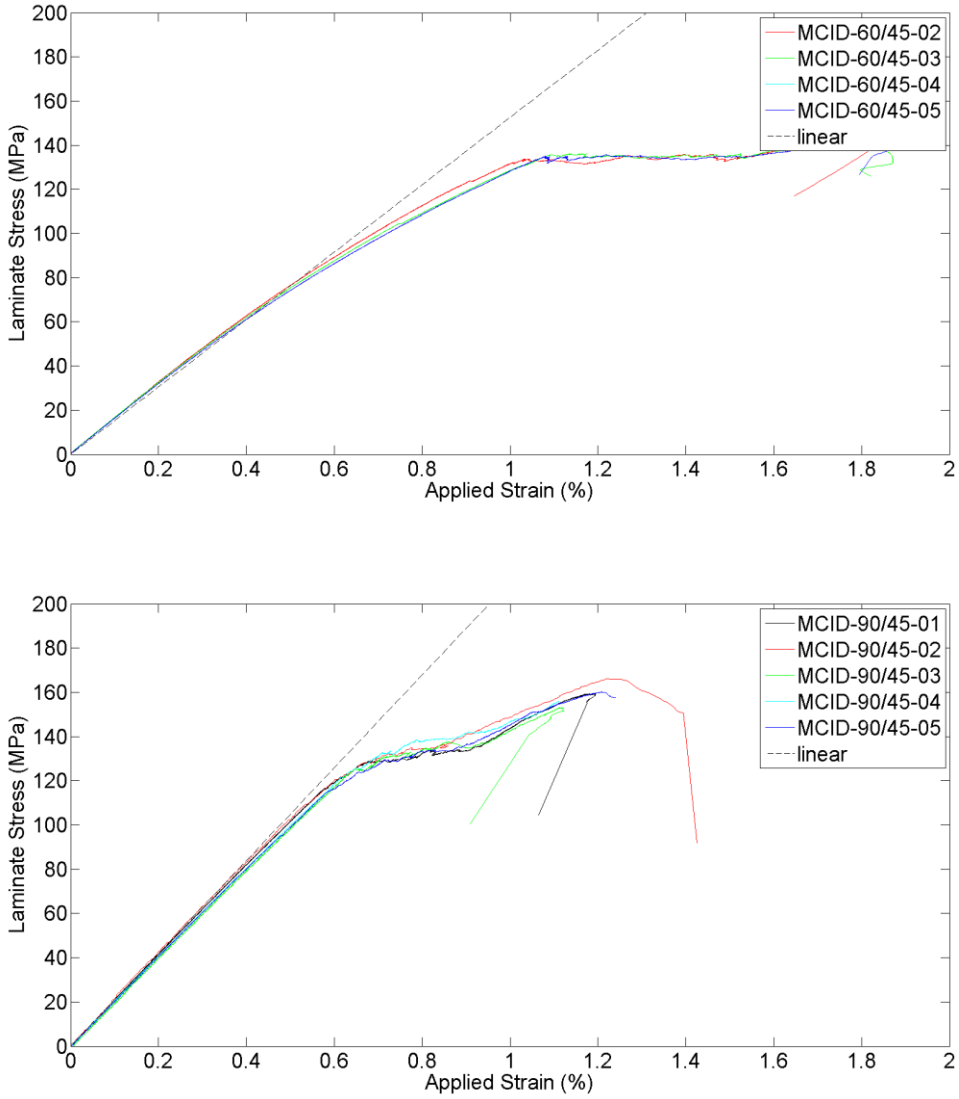

Figure 3.3 Stress-strain curves obtained for $[45_2/-45_2/-60_4/45_2/-45_2/60_4]_s$(MCID-60/45) and $[45_2/-45_2/90_4/45_2/-45_2/90_4]_s$(MCID-90/45) layups.

A summary of the failure stresses obtained for the different laminates is given in Table 3.2. The analysis of the COV given in Table 3.2 highlights the good repeatability of MCID-45-c3, MCID-60/45 and MCID-90/45 specimen series, having COV values

lower than 3.5% for all the cases. In contrast, for MCID-60-c3 the COV was nearly the 10% and for MCID-60-c4 series the highest COV value was obtained (16.40%). It is worth to mention that for these two batches there was a very small scatter in the shape of the stress-strain curves and only differed in the final failure. Additional information about the failure process is shown in the next section.

Specimen Series	Failure stress (MPa)	Standard deviation (MPa)	COV(%)
MCID-45-c3	111.77	2.30	2.05
MCID-60-c3	79.20	7.71	9.73
MCID-60-c4	69.82	11.44	16.40
MCID-60/45	134.02	1.58	1.18
MCID-90/45	130.75	4.38	3.35

Table 3.2 Experimental failure stress

3.3.2 Damage mechanisms

The tested lay-ups presented two different damage mechanisms before failure: transverse cracking and matrix crack induced delamination. From the analysis of the pictures taken during the test, it could be determined that the occurrence of the different damage mechanisms took place in two different ways. The first one was the simultaneous creation of a matrix crack and adjacent delaminations. Indeed, for MCID-60-c3 and MCID-60-c4 layups a sudden failure occurred after the onset of the first delamination induced by matrix cracking (see Figure 3.5). The second one was the accumulation of different damage mechanisms before specimen's failure (they occurred sequentially). In this latter case, the first damage mechanism to appear was matrix cracking. Crack density increased gradually with the applied load and at a certain load level, delaminations began at different interfaces; then growing until final failure (see Figure 3.6-3.7). This behaviour was observed for MCID-60/45 and MCID-90/45 lay-ups. A detailed analysis of the damage occurrence on the different layups is given next.

For MCID-45-c3 series, the first matrix crack appeared at around 110 MPa and it was automatically followed by a delamination. After the occurrence of the first matrix crack in some cases the specimen suddenly failed (specimens 04 and 05), while in the remaining cases (specimens 01, 02 and 03) there was a very large increase of the specimen's elongation before failure. During this interval some new matrix cracks and delaminations appeared, however, they were localized. For example, for specimen MCID-45-c3-03 shown in Figure 3.4, only two zones with a set of cracks were seen in the 50 mm observed zone. It is also worth mentioning that the apparition of new matrix cracks was always simultaneous with delaminations.

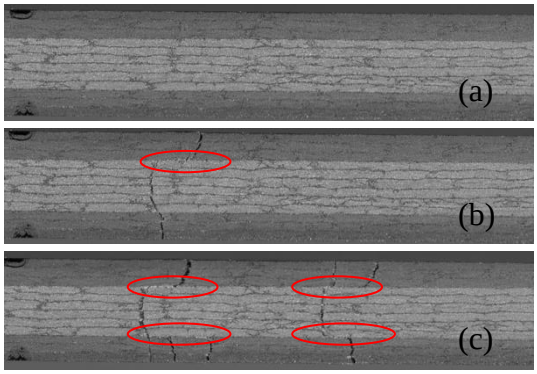

Figure 3.4 Damage process observed in MCID-45-c3-03 specimen ($[45_3/\text{-}45_3]_s$). Circled regions indicate the presence of a delamination. (a) Laminate stress just before the damage initiation σ_{lam}= 110 MPa and applied strain ε_{lam}= 1.1%, (b) just after the damage initiation σ_{lam}= 108.6 MPa and ε_{lam}= 1.14%, (c) just before the failure of the specimen σ_{lam}= 105.31 MPa and ε_{lam}= 1.44%.

For lay-ups $[60_3/\text{-}60_3]_s$ and $[60_4/\text{-}60_4]_s$ (MCID-60-c3 and MCID-60-c4 series), a similar behavior was observed. The specimen failure suddenly happened after the occurrence of delamination, and this delamination appeared just after the presence of a matrix crack. This behavior is shown in Figure 3.5, where the two last pictures captured during the tests of specimens MCID-60-c3-01 and MCID-60-c3-04 are given (see Figures 5b and 5d respectively). It is also observed that the matrix cracks always appeared at the outer layers and that there was a large scatter in the apparition of the first matrix cracks in the different specimens.

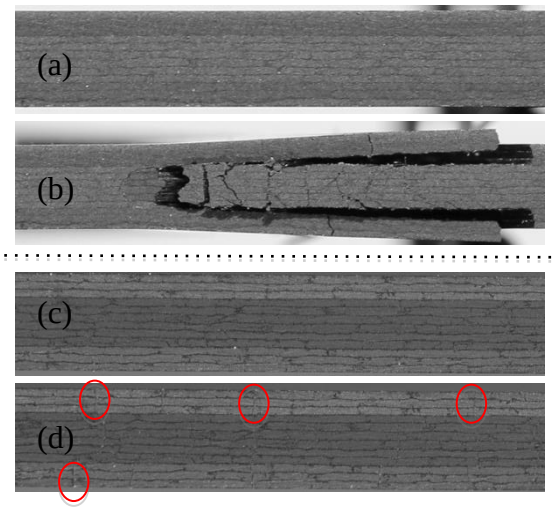

Figure 3.5 Damage process observed in MCID-60-c3-03 specimens ($[60_3/\text{-}60_3]_s$). Circled regions indicate the presence of a matrix crack. Pictures (a) and (b) are of specimen MCID-60-04: (a) for a laminate stress σ_{lam}= 74 MPa and applied strain ε_{lam}= 0.89%, (b) failed specimen (ε_{lam}> 0.89%). Pictures (c) and (d) are of specimen MCID-60-01: (c) σ_{lam}= 89 MPa and ε_{lam}= 1.13%, (d) failed specimen (ε_{lam}> 1.13%) (specimen failure occurred outside the region captured by the camera).

The failure process observed for lay-ups $[45_2/\text{-}45_2/\text{-}60_4/45_2/\text{-}45_2/60_4]_s$ and $[45_2/\text{-}45_2/90_4/45_2/\text{-}45_2/90_4]_s$ is far more complex. For lay-up $[45_2/\text{-}45_2/\text{-}60_4/45_2/\text{-}45_2/60_4]_s$ the first matrix crack was observed at the internal layer (60º) at around 134 MPa and at a laminate strain of 1.05%, Figure 3.6 (a). This was followed by a progressive increase of crack density in the same layer together with the apparition of several cracks in the layers at -60º and 45º, Figure 3.6 (b). During this process of matrix cracking the specimen suffered a large elongation without increasing the laminate stress. This behaviour was followed by a large delamination that promoted specimen failure (around a deformation of 1.8%), Figure 3.6 (c) and (d). These large delaminations mainly appeared at the interface between +45º and -45º plies.

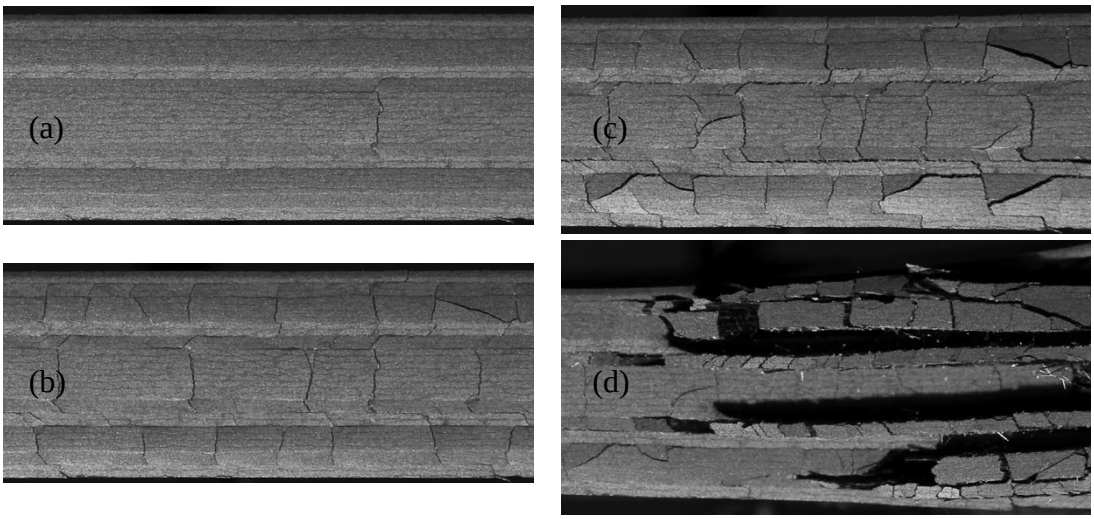

Figure 3.6 Damage process observed in MCID-60/45-04 specimen ($[45_2/-45_2/-60_4/45_2/-45_2/60_4]_s$): (a) just after the damage initiation for a laminate stress σ_{lam}= 134.6 MPa and applied strain ε_{lam}= 1.08%, (b) σ_{lam}= 134 MPa and ε_{lam}= 1.53%, (c) σ_{lam}= 141.1 MPa and ε_{lam}= 1.84%, (d) failed specimen (ε_{lam}> 1.84%).

The damage accumulation process observed for lay-up $[45_2/-45_2/90_4/45_2/-45_2/90_4]_s$ follows the same sequence than lay-up $[45_2/-45_2/-60_4/45_2/-45_2/60_4]_s$ but there is a remarkable difference which is the increase of the loading capacity after matrix crack saturation of the 90 degree plies. The first matrix crack appeared at the central layer for a laminate stress around 126 MPa and a laminate strain around 0.65% (Figure 3.7 (a)). After this, as it was observed for the $[45_2/-45_2/-60_4/45_2/-45_2/60_4]_s$ lay-up, a progressive apparition of matrix cracks at the 90º layers was observed. During this stage the stress remained more or less constant as the specimen elongated (Figure 3.7 (b)). A very large increase on the laminate strain was achieved when this matrix cracking process saturated (strain around 0.9%). However, unlike the $[45_2/-45_2/-60_4/45_2/-45_2/60_4]_s$ laminate, an increase of the laminate stress with the applied strain was observed at this point, as shown in Figure 3.3. Some matrix cracks appeared in the plies oriented at 45º during this stage (Figure 3.7 (c)). This increase on the laminate stress ceased with the occurrence of delamination cracks at the interface between +45º and -45º plies, for a laminate stress of around 155 MPa and applied strain around 1.2% (for example, a delamination crack is observed in the upper right corner of Figure 3.7(c)). Specimens' failure occurred just after the apparition of these delamination cracks (Figure 3.7 (d)).

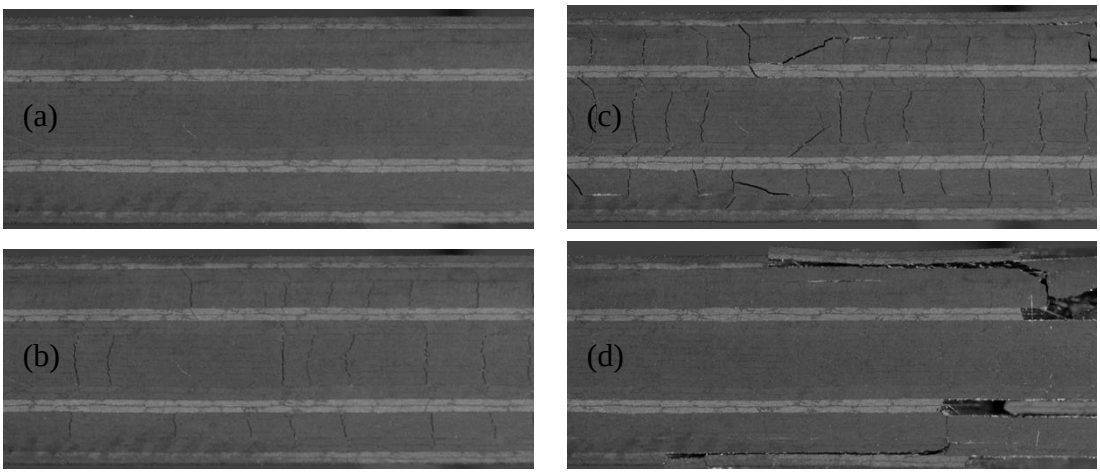

Figure 3.7 Damage process observed in MCID-90/45-01 specimen ([452/-452/904/452/-452/904]s): (a) just before the damage initiation for a laminate stress σ_{lam}= 126MPa and applied strain ε_{lam}= 0.65%, (b) after the damage initiation σlam= 133 MPa and ε_{lam}= 0.85%, (c) just before the specimen rupture σ_{lam}= 159 MPa and εlam= 1.17%, (d) failed specimen (ε_{lam}> 1.17%).

It is worth noting the influence of the ply thickness and the orientation of the layers on the damage occurrence. Laminates MCID-60-c3 and MCID-60-c4 have the same stacking sequence but different ply clustering (3 and 4). It is observed that the laminates with higher clustering (MCID-60-c4) failed at lower stress levels. The difference on the failure stress of MCID-60-c3 and MCID-60-c4 is of 10 MPa, which corresponds to almost a decrease of a 15%. The failure modes observed in both specimen sets are identical, which correspond to a sudden matrix cracking, an immediate delamination and the failure of the specimen. However, for laminates with higher ply clustering (n=4), the scatter in the apparition of the first matrix crack is higher, besides the lower strength. This phenomenon is captured by the COV given in Table 3.2, which is higher for n=4 than for n=3.

Another interesting comparison is between laminates MCID-60-c3 and MCID-45-c3, which have the same number of plies but different ply orientations (60º and 45º respectively). The loading capacity in this case is higher for MCID-45-c3 lay-ups and the laminate strain at peak load is slightly higher for MCID-60-c3 lay-ups. There is a difference of the maximum laminate stress of 31 MPa (around a 40%). As seen in figures 3.2 and 3.3 the failure mode is similar for both lay-ups: sudden delaminations appear simultaneously just after the first matrix cracks and cause specimen failure.

Finally, the results obtained with the MCID-60/45 laminate can be compared with the results obtained with the MCID-60-c4 laminate. Both have the same ply clustering of the 60º plies (4 outer plies and 8 plies in the centre), but for MCID-60/45 lay-up the laminas oriented $\pm 60^{o}$ are placed in between +45/-45 plies. The failure stress obtained for MCID-60-c4 laminate was almost half of the failure stress of MCID-60/45 laminate.

3.4 Discussion

Matrix dominated failure mechanisms drove specimen's failure in the different lay-ups tested in the experimental campaign. In some specimens, several matrix cracks appeared at different layers before promoting the specimen's failure due to the growth of an interlaminar crack. Among the rest of the specimens, the apparition of the first matrix crack immediately promoted delamination growth and the specimen's failure. It is worth to analysing whether the occurrence of the different damage mechanisms in the different plies of the laminate is foreseeable with existing criteria or not. Regarding matrix crack induced delamination (MCID), these authors have recently developed a failure criterion [7], as briefly explained in the introduction. This failure criterion evaluates whether the presence of a matrix crack in a ply may actually promote delamination growth at the interface with neighbouring plies. This failure criterion is sensitive to the thickness and location of the ply within the laminate. It is written in terms of local ply stresses and can be used to compute the laminate stress required to cause failure of a specific ply failure in the laminate containing a matrix crack.

3.4.1 Formulation and implementation of the MCID criterion

The failure criterion for MCID reads:

$$\left(\frac{\sigma_{11}}{X_1^{MD}}\right)^2 + \left(\frac{\sigma_{22}}{X_2^{MD}}\right)^2 + \left(\frac{\sigma_{12}}{X_6^{MD}}\right)^2 + \frac{\sigma_{11}\sigma_{12}}{X_{16}^{MD}} + \frac{\sigma_{22}\sigma_{12}}{X_{26}^{MD}} + \frac{\sigma_{11}\sigma_{22}}{X_{12}^{MD}} = 1 \qquad (1)$$

where σ_{11} is the ply stress in the fibre direction, σ_{22} is the ply stress in the transverse direction and σ_{12} is the ply shear stress. All three stresses are measured in local ply axes.

Parameters X_k^{MD} and X_{kl}^{MD} depend on the location of the ply within the laminate, the fracture toughness of the interface and the elastic properties of the laminate:

$$X_k^{MD} = \sqrt{\frac{2m\mathcal{G}_c}{\chi_{kk}}} \tag{2}$$

$$X_{kl}^{MD} = \frac{2m\mathcal{G}_c}{(\chi_{kl}+\chi_{lk})} \tag{3}$$

Being m the position of the ply within the laminate, $\mathcal{G}_c$ the critical energy release rate for mode II-III delamination growth, and χ_{kl} the components of the matrix:

$$\chi = S^T A^T \bar{a} A S \tag{4}$$

where *S* is the ply compliance matrix in local axes, *A* is the laminate stiffness matrix obtained using classical laminate theory and $\bar{a}$ is the computation of the difference of the inverse matrix ABD matrix of the undamaged and damaged laminated. Further details can be found in [7].

The MCID criterion assumes the existence of a crack in the matrix Therefore, to completely analyse the occurrence of the different failure mechanisms observed in the tests, a failure criterion for matrix cracking is also needed. Among the several failure criteria for transverse cracking available in the literature [6] the LaRC03 [13] has been used here as it accounts for the influence of the ply thickness.

The failure criterion given in Equation (1) and the LaRC03 criterion for transverse cracking have been implemented as a UVARM user subroutine for ABAQUS® [15]. The different specimens tested in the experimental campaign have been simulated using laminated S4 elements and the material properties listed in Table 3.3. In order to evaluate the failure criteria selected at the different plies of the specimen, a displacement has been applied to the specimen on one side while the opposite side was clamped. Therefore, the failure load of each ply for the different failure mechanisms is obtained.

Material properties (units)	Value
E_1 (MPa)	134700[16]
E_2 (MPa)	7700 [16]
G_{12} (MPa)	4200 [16]
υ_{12}	0.367 [16]
$\mathcal{G}_{Ic}$(J/m^2)	0.24 [17]
$\mathcal{G}_{IIc}$(J/m^2)	0.74 [17]*
Ply thickness (mm)	0.1875

Table 3.3 T800-M21 material properties taken from references [16] and [17].

3.4.2 Analysis of results

For each lay-up sequence, the laminate stresses of each ply obtained for matrix cracking (TC) and matrix cracking induced delamination (MCID) failures are listed in Table 3.4.

Laminate stresses (MPa)						
Ply	Damage mechanism	MCID-45-c3 $[45_3/-45_3]_s$	MCID-60-c3 $[60_3/-60_3]_s$	MCID-60-c4 $[60_4/-60_4]_s$	MCID-60/45 $[45_2/-45_2/-60_4/45_2/-45_2/60_4]_s$	MCID-90/45 $[45_2/-45_2/90_4/45_2/-45_2/90_4]_s$
1	MCID	87.9	83.6	72.4	166.8	165.9
	TC	126.9	59.6	59.6	132.4	174.7
2	MCID	105.8	103.4	89.6	245.1	235.9
	TC	159.9	86.7	86.7	173.6	241.9
3	MCID	-	-	-	226.8	275.1
	TC	-	-	-	145.4	188.2
4	MCID	-	-	-	279.4	295.7
	TC	-	-	-	173.6	241.9

5	MCID	-	-	-	283.4	300.5
	TC	-	-	-	173.6	241.9
6	MCID	-	-	-	166.5	218.5
	TC	-	-	-	145.4	188.2

Table 3.4 Numerical model prediction for matrix cracking and delamination onset.

It can be observed in Table 3.4 that for laminates MCID-45-c3, MCID-60-c3 and MCID-60-c4, the failure criteria predict that the first matrix cracks appear at the outer layer. For these laminates, matrix-cracking induced delamination is predicted at a lower stress than the transverse cracking. Therefore, and according to the numerical predictions, when a matrix crack appears at the outer plies this will immediately induce a delamination at the interface. This is in agreement with the observations in the experimental tests; as explained in the previous section, the apparition of matrix cracks and delamination was almost simultaneous, especially for the MCID-60-c3 and MCID-60-c4 specimens.

On the other hand, for the MCID-45-c3 laminates, the predicted laminate stress for transverse cracking of the outer layer is very high compared to the experimental value in which the first matrix cracks were observed. Moreover, transverse cracking occurred at a higher laminate stress than for MCID, and therefore, there were no transverse cracks in the matrix to actually trigger delamination for the laminate stress predicted with the MCID criterion. MCID was fulfilled once matrix cracks appear in the material and delamination occurs instantaneously.

The results of the experimental and predicted laminate failure stress for both phenomena, matrix cracking and MCID, are plotted in Figure 3.8. Only the minimum values of the laminate stresses for each configuration are included.

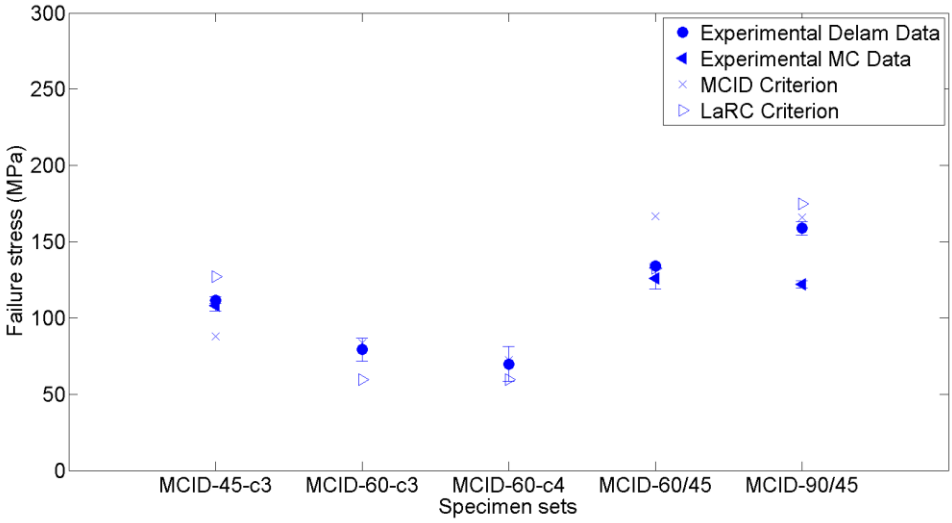

Figure 3.8 Model prediction and experimental results

In the case of specimens MCID-60-c3 and MCID-60-c4, the predicted onset for matrix cracking is at the same value (59.61 MPa). However, this is again not in agreement with the experimental observations, where a large scatter in the apparition of matrix cracks was observed. In contrast, for delamination onset, according to numerical predictions, layers with higher ply clustering will fail with a lower applied load (9 MPa lower), making the high-clustered laminates more prone to delamination failure. The difference observed in the experiments between both laminates (MCID-60-c3 and MCID-60-c4) was around 10 MPa, matching the predictions.

Finally, the MCID-60/45 and MCID-90/45 specimen sets have more interfaces and plies with different orientations. In the case of MCID-60/45, and according to the numerical predictions, matrix cracks should appear before delamination with a difference of 30 MPa. However, the analysis of the pictures showed that a large number of cracks at the ±60 plies appeared followed by small delamination onset at their tips. The load carrying capacity was constant after the appearance of the first matrix cracks, and when delamination appeared at the interface between +45 and -45 plies, the specimen failed. In this case, the difference between the LaRC criterion and the observed strain is negligible. The MCID criterion, however, overpredicts the experimental observations (around 25%). The authors attribute this difference to the fact

that MCID was not actually observed in these specimens and specimen failure was in fact driven by matrix cracking.

In the case of the MCID-90/45 specimens, matrix cracks were observed for lower loads than those predicted by the LaRC criterion. Matrix cracks appear in the 90º plies for loads of a stress value around 45% lower than what had been numerically predicted. Moreover, these matrix cracks where followed by very small delaminations that appeared at the matrix crack tips, but they did not grow. Contrary to the MCID-60/45 laminates, in the MCID-90/45 specimens the matrix cracking process was not driving the failure process at all after the saturation of the matrix cracks at the 90º layers, in fact the specimens were able to carry more load until the apparition of a delamination crack at the interface between +45 and -45 plies and the specimen failure was mainly driven by these delaminations. The MCID failure stress predicted with the MCID failure criterion is around 166 MPa and the experimental load around 160 MPa. Therefore, a good agreement between numerical and experimental predictions is obtained with the MCID criterion.

To sum up, the MCID criterion used to predict the specimen behaviour properly locates the most critical plies to delaminate. It takes into account the different variables, such as the stacking sequence and the ply clustering. The predictions are in agreement with the experimental data in the case where matrix cracking is the first damage mechanism to occur. Moreover, for some laminates MCID may also appear at a lower load than when the first matrix crack is created, provided that there are some pre-existing cracks in the laminate. This is also captured by the MCID failure criterion, and in these situations, if there are no pre-existing cracks in the laminate, specimen failure will happen as soon as the first matrix crack appears. Within this scope, it is worth mentioning that the prediction of transverse cracking using the LaRC criteria has been shown not to be accurate for some of the explored laminates.

3.5 Conclusions

An experimental campaign has been designed to analyse the occurrence and progression of transverse cracks and delaminations induced by matrix cracking. To this end, five different lay-ups have been chosen and the damage onset and evolution in the different plies have been analysed.

In general terms, good repeatability between the different specimens of the batch has been obtained. MCID-60-c3 and MCID-60-c4 also had good repeatability in the mechanical behaviour, but with a COV of 9.6% and 16.4% in strength. Additionally, from the chosen lay-ups, four of the five tested laminates failed due to the growth of matrix crack induced delaminations while, for one of the laminates, specimen failure was driven by the large number of matrix cracks in the different plies.

Furthermore, the failure criterion previously developed by the authors to predict delamination onset for matrix crack has been used to analyse and discuss the experimental observations. The onset of transverse cracks are predicted using the LaRC failure criterion whereas the matrix crack induced delamination is analyzed by means of the recently developed MCID criterion. The predictions of the MCID failure criterion were in accordance with the experimental observations. The failure criterion accurately predicted the location of the delamination cracks and a good agreement in the predicted failure stresses was obtained.

Acknowledgements

This work was funded by AIRBUS under project iComp – the integrated method for the structural design of Composite components. The authors gratefully acknowledge the support provided by AIRBUS, along with the support of the Spanish government through DG-CICYT under contract DPI2012-34465 and MAT2012-37552-C03-03.

References

[1] Crossman FW and Wang ASD. The dependence of the transverse cracking and delamination on ply thickness in graphite/epoxy laminates. Damage in Composite Materials. ASTM STP 1982; 775:118-39.

[2] Johnson P and Chang F. Characterization of matrix crack induced failure - Part I: Experiments. Journal of Composite Materials 2001; 35(22):2009-35.

[3] Johnson P and Chang F. Characterization of matrix crack induced failure - Part II: Analysis and verifications. Journal of Composite Materials 2001; 35(22):2037-74.

[4] Hallett SR, Jiang W, Khan B and Wisnom MR. Modelling the interaction between matrix cracks and delamination damage in scaled quasi-isotropic specimens. Composite Science and Technology 2008;68(1):80-9.

[5] Guillamet G, Turon A, Costa J, Renart J, Linde P, Mayugo JA., Damage occurrence at edges of Non-crimp-fabric thin-ply laminates under off-axis uniaxial loading. Composites Science and Technology, forthcoming (2014).

[6] Orifici AC, Herszberg I, Thomson RS. Review of methodologies for composite material modelling incorporating failure. Composite Structures 2008;86(2):194–210.

[7]Zubillaga L, Turon A, Maimí P, Costa J, Mahdi S and Linde P. An energy based failure criterion for matrix crack induced delamination in laminated composite structures. Composite Structures 2014; 112:339-344.

[8] O'Brien TK. Analysis of local delaminations and their influence on composite laminate behaviour. NASA Technical Memorandum 85728. 1984.

[9] Maimí P, Camanho PP, Mayugo JA, Turon A. Matrix cracking and delamination in laminated composites. Part I: Ply constitutive law, first ply failure and onset of delamination. Mech Mater 2011;43(4):169–85.

[10] Hallett S.R., Green B.G., Jiang W.G., Wisnom M.R., An experimental and numerical investigation into the damage mechanisms in notched composite. Composites: Part A 40 (2009) 613–624.

[11] Van Der Meer FP, Sluys LJ. Continuum models for the analysis of progressive failure in composite laminates. J Compos Mater 2009;43(20):2131–56.

[12] Iarve E, Gurvich M, Mollenhauer D, Rose CA, Dávila CG. Mesh-independent matrix cracking and delamination modeling in laminated composites. International Journal for Numerical Methods in Engineering, 2011;88(8):749–73.

[13] Camanho PP, Dávila CG, Pinho ST, Iannucci L, Robinson P. Prediction of in situ strengths and matrix cracking in composites under transverse tension and in-plane shear. Composites Part A: Applied Science and Manufacturing, 2006;37(2):165–76.

[14] Sebaey TA, Costa J, Maimí P, Batista Y, Blanco N, Mayugo JA, Measurement of the in situ transverse tensile strength of composite plies by means of the real time monitoring of microcracking, Composites Part B: Engineering, in Press, http://dx.doi.org/10.1016/j.compositesb.2014.02.001.

[15] ABAQUS 6.11 User manual.

[16] Marín L, Trias D, Badalló P, Rus G and Mayugo JA. Optimization of composite stiffened panels under mechanical and hygrothermal loads using neural networks and genetic algorithms. Composite Structures 2012; 94:3321-3326

[17] Mayugo JA. Proyecto: ensayo virtual y supervisión estructural de revestimientos reforzados con larguerillos de fibra de carbono EVISER IT-01, ref: TRA2006-15718-C02-01/TAIR. AMADE. Universitat de Girona; 2006‑2009.

4 Experimental and numerical analysis of free-edge delamination by means of a two-fold criterion and a cohesive zone model

L. Zubillaga, N. Carrere, A. Turon, G. Guillamet, P. Linde. “Experimental and numerical analysis of free-edge delamination by means of a two-fold criterion and a cohesive zone model”. Submitted to *Composite Part A: Applied Science and Manufacturing*.

http://www.journals.elsevier.com/composites-part-a-applied-science-and-manufacturing/

Abstract

This work aims to predict free-edge delamination. To this purpose a comparison between two existing models from the literature has been made. On one hand, a coupled criterion based on a combination of an energy criterion and a stress criterion was used, whereas, on the other hand, a cohesive zone model that assumes a quasibrittle behavior of the interface was employed. Additionally, an experimental campaign was performed using 5 different T800/M21 lay-ups. Finally, the experimental results and the predictions were compared. A good correlation was found between the experimental data and the predictions, with the cohesive models offering a slightly better approach.

5 Conclusions

5.1 Introduction

Laminated composites, such as carbon fiber reinforced polymer (CFRP), have been introduced in the transportation industry substituting classical metallic materials such as aluminum and steel. The higher tensile strength with lower weight (great strength/weight ratio) promotes their use in high-tech applications.

Many research works has been done in order to have a better understanding of the mechanical behavior of these materials and to develop the proper models to predict their mechanical/structural behavior under working conditions. In the literature, different models are proposed to predict the different damage mechanisms that can occur in laminated composites. Most of them are suitable for the first design steps. However, in the case of delamination, although there exist different models to predict delamination in laminated composite structures, there is a lack of appropriate models to predict delamination in an efficient manner (i.e. short computational time) and therefore, to account for them in the design of laminated composites.

Among the different sources for delamination onset and growth, matrix crack induced delamination and delamination induced by free-edge effects have been deeply analyzed in this work. The analysis has covered the experimental observation of both phenomena, with dedicated test campaigns focused on each of the two sources of delamination, and a numerical prediction by the development of two different analysis tools mostly based on Fracture Mechanics principles.

5.2 Matrix crack induced delamination

A procedure to account for matrix crack induced delamination has been developed in this work. The procedure determines the existence of matrix cracks at every ply of the laminate and, in the case of existence, the onset of delamination from their tips. The prediction of the cracking is based on LaRC'03 criterion and the matrix crack induced delamination criterion has been developed in this work based on Fracture Mechanics principles by comparing the available elastic energy on the laminate with the presence of a matrix crack and the fracture toughness of the interface. The computation of the

available energy is made using Classical Laminate Theory but taking into account the stiffness reduction due to the presence of a matrix crack.

The prediction of the MCID model has been initially compared to experimental data available in the literature. Moreover, an experimental campaign has been defined and performed to observe matrix cracking induced delamination in specimens loaded in tension.The occurrence of the different failure mechanisms during the loading of the specimens has been monitored in the experiments. Therefore, the critical laminate stress for matrix cracking and delamination have been obtained.The experimental data available in the literature and the data obtained in the test campaign are in accordance with the model predictions.

Moreover, the model has been implemented in a finite element software as a post-processing tool, and due to the lack in the literature of general models to account for matrix cracking induced delamination, the failure criterion proposed in this work could be incorporated into a wider set of failure criteria for composites, for instance LaRC or Puck criteria.

The most relevant conclusions from the matrix cracking induced delamination analysis presented in chapter 2 and 3 can be summarized as follows:

- The parameters of the failure criterion are dependent on material properties, ply thickness and laminate compliance properties before and after the presence of a matrix crack.

- A good agreement has been obtained between the proposed model to determine matrix crack induced delamination and the experimental data available in literature.

- The MCID failure criterion accurately predicted the location of the delamination cracks and a good agreement in the predicted failure stresses has been obtained.

- The influence of the ply thickness was observed, both, experimentally and analytically, concluding an inverse relationship between the lamina/ply thickness and the delamination resistance.

- The predictions of the LaRC failure criterion for matrix cracking have not been very accurate nor the location of the matrix cracks with respect the experimental observations in the tests.

- It has been demonstrated that, for certain laminate configurations, the failure load predicted for MCID is lower than that of fiber failure and matrix cracking. This provides evidence of the convenience of taking MCID into account when designing laminated structures.

5.3 Free-edge delamination

Two different models have been compared for the suitability to predict free-edge delamination.

On the one hand, a coupled criterion that considers two conditions that should be fulfilled in order to promote the delamination. The first condition is an energy condition that verifies if there is enough energy stored in the material to promote delamination propagation and the second condition is a stress condition that compares the local stress state with the resistance of the material.

On the other hand, the cohesive zone model approach has been used to predict both delamination onset and growth, by means of a mixed-mode interaction model formulated as a function of the strength and fracture toughness of the interface.

Additionally, an experimental test campaign has been performed to obtain the failure resistance of specimens for free-edge delamination. Finally, the comparison between both models and the obtained experimental data has been done to analyze the suitability of both approaches to predict free-edge delamination and to choose the best method to determine delamination onset at free-edges at early design steps.

The most relevant conclusions from the free edge delamination analysis presented in chapter 4 can be summarized as follows:

- An experimental test matrix has been defined to study the influence of ply blocking and mismatch angle.

- An inverse relationship is found between the thickness of the lamina and the delamination resistance from the free-edges.

- The greater the angle mismatch with respect the applied load the lower the loading capacity of the material.

-Both approaches, FFM and cohesive zone model, predict properly the failure threshold for all the tested lay-ups.However, cohesive elements give a more accurate approach than the coupled criterion.

- In terms of computational effort, a very efficient finite element model has been developed, applying generalized plane strain conditions. Using this efficient model, the prediction using cohesive zone elements is faster than the prediction using the FFM approach. The coupled criterion requires the computation of the stress distribution and available energy release rate, along the potential delamination growth path, using several FEM models. Even though, for more complex structures cohesive element models should be more expensive computationally than the application of the threshold values obtained by the coupled criterion as a point stress criterion.

In conclusion, both criteria are adequate for predicting delamination at free-edges. In general terms, the coupled criterion is more efficient for large parts or structures as it can be applied as a point stress criterion. In contrast, for simple test coupons the prediction made with cohesive elements is more efficient.

5.4 Future work

Based on the results of this research and the conducted literature review, the following points are proposed as future work:

-A deeper study of the different failure criteria available in the literature to predict matrix cracking should be performed. A comparison of the different formulations with

the experimental results obtained in this work will highlight the convenience or not of developing a new failure criterion for matrix cracking.

- The matrix crack induced delamination has been developed assuming in-plane loading. However, in a general case, bending loads can also be present. A generalization of the MCID failure criterion to also account bending loads should be addressed, together with an experimental campaign to validate the model under flexural loads.

-To monitor the damage occurrence during the experimental tests, pictures of the specimen edge have been taken continuously. Matrix and delamination cracks at the free edge of the specimen have been identified with this technique, but it is not possible to know whether or not the observed cracks span the width of the specimens. Other experimental techniques such as X-ray or tomography should be considered to perform a deeper analysis of the experimental behavior. The applicability of an acoustic emission system is also worth to be considered for future test campaigns.

- The implementation of the coupled criterion as a point stress criterion. The point stress criterion is based on the measurement of the stress at a critical length from the singularity. In the cause of free-edge delamination, the measurements should be done at a critical length from the edge of the specimen. The coupled criterion gives both values the nucleation length which corresponds with the critical length where measurements of the critical stress that is also obtained by the coupled criterion should be measured. A very refined mesh at the edges of the parts is required, thus increasing the computational cost, to apply the coupled criterion. Therefore, a study of the optimal transition between a fine mesh at the edges and a coarser mesh in the inner regions of the structure should be addressed to reduce computational effort. Additionally to the guidelines for defining the proper mesh, it is also needed the implementation of a subroutine to automatize the post-processing of the nodal stresses at the critical point and compare it with the stress threshold and predict delamination growth.

Appendix

Post-processing tool for delamination hot-spot location using ABAQUS with a UVARM subroutine.

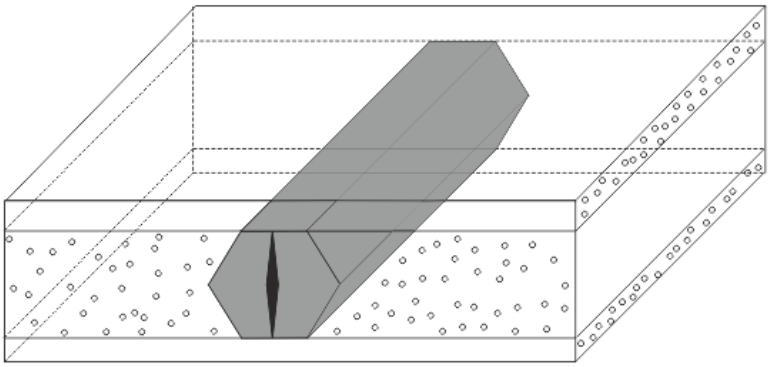

AMADE Composite Research Group

University of Girona, Spain

USER MANUAL

DELAM-UVARM.V3

Post-processing tool for delamination onset hot-spot location using ABAQUS with a UVARM subroutine.

Lierni Zubillaga [(a)]

Albert Turon [(a)]

Pere Maimí [(a)]

Josep Costa [(a)]

Version 3.0

[(a)] AMADE, Polytechnic School, University of Girona,Campus Montilivi s/n, 17071,

Girona, Spain

Table of contents

Introduction

The objective of the MCID.for UVARM subroutine presented here is to determine the hot-spots of a laminated composite structure for matrix crack induced delamination failure. For this purpose two different criteria have been implemented. Firstly, LaRC criteria [1] to determine if the matrix is cracked and secondly, MCID [2] criterion to determine if the delamination has initiated. The MCID.for UVARM subroutine can be used in ABAQUS/Standard as a post-processing tool, to compute a delamination and matrix cracking failure index at each integration point of the model for each substep of the analysis.

Limitations of the current version

The formulation used in the v3 version does not account for mode I effects. Delamination running under mixed-mode II-III load is only predicted.

Delamination failure criteria is computed using the stress-state of each integration point of an uncracked laminate. The change on the laminate stiffness due to the delamination and or matrix cracks is not considered in the FE model. Therefore, it is recommended to use the subroutine as a “locator” of hot-spot regions and then perform a detailed analysis of this region using an advanced tool such as the cohesive zone elements.

Theoretical background

Delamination triggered by matrix cracks needs to take into account two different phenomena: the cracking of the matrix and delamination caused by the propagation of the matrix crack within the interface between the cracked and neighboring plies. The proposed implementation considers the two phenomena independently. Firstly, matrix cracking is evaluated by the criterion of LaRC [1] and then delamination onset is determined by a criterion based on the elastic energy stored in the lamina [2].

Matrix Cracking (LaRC)

Matrix cracking depends on the orientation of the fibers and the loading conditions, because of that the criterion should be applied at each ply. The used criterion is applicable when the loading condition are transverse tension and in plane shear. The criterion is based on Linear Fracture Mechanics and assumes that the cracks grow self-similarly, the orientation of the crack is in the principal directions of elastic symmetry of an orthotropic ply and that the stress intensity factors are related to energy release rates. The proposed criterion for matrix cracking reads [1]:

$$(1-\mathrm{g})\frac{\sigma_{22}}{Y_{is}^{T}}+\mathrm{g}\left(\frac{\sigma_{22}}{Y_{is}^{T}}\right)^{2}+\left(\frac{\sigma_{12}}{S_{is}^{L}}\right)^{2}\leq 1 \qquad (1)$$

where g is the relation between the fracture toughness in mode I and mode II GIc/GIIc, σ_{22} is the stress in local axis in the direction perpendicular to the fiber, σ_{12} is the shear in plane component in local axis. Y^{T}_{is} is the matrix in-situ strength for transverse loading and S^{L}_{is} the in-situ strength correspondent to the shear loading.

Delamination triggered by matrix cracks (MCID)

The criterion is based on a previous work [3,4] were energy based criteria are proposed considering Fracture Mechanics. The failure criterion is obtained by comparing the elastic energy released in a laminate due to the increase of delaminated area (s in Figure 3.1) and the fracture toughness of the interface between plies.

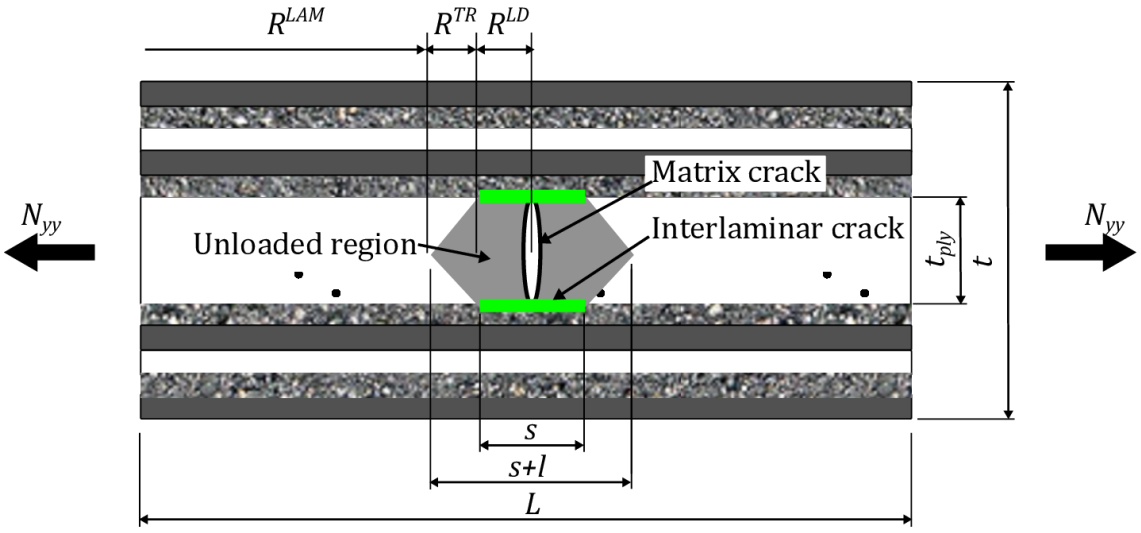

Figure 1 Longitudinal section of an uncracked and cracked laminate under tension. The presence of a matrix crack induces a transition region to recover the ply far-field stress.

The failure criterion for MCID that reads:

$$\left(\frac{\sigma_{11}}{X_1^{MD}}\right)^2 + \left(\frac{\sigma_{22}}{X_2^{MD}}\right)^2 + \left(\frac{\sigma_{12}}{X_6^{MD}}\right)^2 + \frac{\sigma_{11}\sigma_{12}}{X_{16}^{MD}} + \frac{\sigma_{22}\sigma_{12}}{X_{26}^{MD}} + \frac{\sigma_{11}\sigma_{22}}{X_{12}^{MD}} = 1 \quad (2)$$

where σ_{11} is the ply stress in the fiber direction, σ_{22} is the ply stress in the transverse direction and σ_{12} is the ply shear stress. All three stresses are measured in local ply axes. Parameters X_k^{MD} and X_{kl}^{MD} depend on the location of the ply within the laminate, the fracture toughness of the interface and the elastic properties of the laminate:

$$X_k^{MD} = \sqrt{\frac{2n\mathcal{G}_c}{\chi_{kk}}} \quad (3)$$

$$X_{kl}^{MD} = \frac{2n\mathcal{G}_c}{(\chi_{kl}+\chi_{lk})} \quad (4)$$

Being n the position of the ply within the laminate, $\mathcal{G}_c$ the critical energy release rate for mode II-III delamination growth, and χ_{kl} the components of the matrix:

$$\chi = S^T A^T \bar{a} A S \quad (5)$$

where *S* is the ply compliance matrix in local axis, *A* is the laminate stiffness matrix obtained using Classical Laminate Theory and $\bar{a}$ is the computation of the difference of the inverse matrix ABDmatrix of the undamaged and damaged laminated. Further details [4].

USER Instructions

The proposed formulation has been implemented in a Fortran subroutine UVARM. Two different files are needed to be created (*jobname.inp* and *jobname.ma*) in order to use the subroutine MCID_v3.for:

ABAQUS Inputs (jobname.inp)

This file is a standard input file for ABAQUS/Standard but contains only few differences and some recommendations:

Shell element type with composite capabilities should be used in the model. It is recommended to have at least 3 integration point at each ply per thickness, for example:

```
*ELEMENT, TYPE=S4
      1,      1,     2,   102,   101,
**
*ELGEN, ELSET=SHELL
      1, 99, 1, 1, 20, 100, 100
*Shell Section, elset=SHELL, composite, orient=or0
0.25, 3, CAR-EPO -0, 0.
1.0, 3, CAR-EPO -C, 90.
0.25, 3, CAR-EPO -0, 0.
```

It is should be noted that a different material has to be created for every ply that has a different material, orientation, and/or ply thickness (if it is symmetrical only one half of the laminate). An *inp example file is given in the appendix to clarify this.

When material properties are defined an additional command line is necessary for each material type. User output variables should be defined. In this case only three output variables are necessary the first one UVARM1 for matrix cracking criterion and UVARM2 (Generalized plane strain condition) and UVARM3 (Generalized plane stress condition) for delamination onset criterion:

```
*Material, name=CAR-EPO-C

*Elastic, type=LAMINA

172000.,8900., 0.35,4200.,4200.,2908.

*USER OUTPUT VARIABLES

 3,
```

Finally to be able to plot the results in the viewer this results should be stored. In the Step part where element output are asked all the integration points in the thickness that are wanted to be stored should be added and the name of the UVARM variable. This command line could be use as much as needed:

```
*OUTPUT, FIELD, FREQ=1
 U,RF
*ELEMENT OUTPUT
E,S
*ELEMENT OUTPUT
1,2,3,4,5,6,7,8,9,10
UVARM, S, E, SSAVG, SE
*ELEMENT OUTPUT
11,12,13,14,15,16,17,18,19,20
UVARM, S, E, SSAVG, SE
**
```

Material properties file. (jobname.ma)

This file will contain the ply properties needed in the subroutine to compute the two failure indexes. These properties are geometrical values such as laminate and ply thickness, and elastic properties of the ply and the laminate. Ply elastic properties of UD lamina are obtained directly from the material datasheet, however the laminate elastic properties need to be computed. To facilitate the calculation of them, a matlab file has been created. This file is explained in the next subsection and given in Appendix I. The final contents of the *jobname.ma* file looks like:

```
** MAT. #1: MATERIAL NAME: Description of the material
   CAR-EPO-O
** E22,       E11,       nu12 ,      G21,    GIc,    GIIc, YTUD, totalthick
   8900.0, 172000.0,   0.35,   4200.0,  0.765,  1.250,41.43, 6.0
** thick,      layers,  SLDAT
   0.375,   11.0,   69.40
** X1co, X2co, X6co, X12co,X16co,X26co
   9671.88, 131.00,   26.69,   640062.21,  -140317.48,  -2046.16
** X1cc, X2cc, X6cc, X12cc,X16cc,X26cc
   11977.52, 183.21,   27.39,   1097209.24,  -164042.71,  -2509.24
** X1phy, X2phy, X6phy, X12phy,X16phy,X26phy
2301.77, 60.10,   19.21,   71223.44,  -26592.13,  -642.40
```

Considerations:

The name of the .ma file should be the same as the .inp file.

```
Stiffner45.inp ----> Stiffner45.ma
```

The lines that starts with ** are not read by the subroutine.

The material name should be in capital letters and should match with the one defined in the input file.

For each material type these 12 lines should be written at the .ma file.

NOTE: In Appendix II there is an example of material definition for each different ply of the laminate.

MATLAB file to generate .ma files

The input parameters to run the matlab file are 8 material properties (per material) and the lay-up of the composite material. The output file of this matlab code is *jobname.ma* and it is generate at the same directory that it is the matlab file.

The material properties are the ones measured for the UD lamina.

```
% E1, E2, nu12, G12 YTUD, SLDAT(MPa) GIc GIIc ()
Mat(1,:)=[172000, 8900, 0.35, 4200, 41.43, 69.4, .765, 1.25];
```

For any additional material only another row should be added to the Mat matrix.

On the other hand the composite lay-up needs 3 parameters: material type, ply orientation and ply thickness.

```
% The lamina need to define material, angle and thickness
L(1,:)=[1, 30, 0.25];
L(2,:)=[1, -30, 0.25];
L(3,:)=[1, 90, 0.5];
```

L matrix contains as many rows as plies has the laminate.

Once these parameters have been introduced in the matlab code, it can be executed. The program searches for different rows at the L matrix and generates a new different 'material type' for each different row. The first material corresponds with the L(1,:). The next material will correspond to the next different row at the L matrix. For example:

```
** MAT. #1: MATERIAL NAME: Description of the material
   MATERIAL NAME IN CAPS
** E22,       E11,       nu12 ,      G21,    GIc,    GIIc, YTUD,totalthick
   8900.0, 172000.0,   0.35,   4200.0,  0.765,  1.250,41.43,6.0
```

```
** thick,      layers,  SLDAT
   0.375,   11.0,   69.40
** X1co, X2co, X6co, X12co,X16co,X26co
   9671.88, 131.00,   26.69,   640062.21,  -140317.48,  -2046.16
** X1cc, X2cc, X6cc, X12cc,X16cc,X26cc
   11977.52, 183.21,   27.39,   1097209.24,  -164042.71,  -2509.24
** X1phy, X2phy, X6phy, X12phy,X16phy,X26phy
   2301.77, 60.10,   19.21,   71223.44,  -26592.13,  -642.40
** MAT. #2: MATERIAL NAME: Description of the material
   MATERIAL NAME IN CAPS
** E22,       E11,       nu12 ,      G21,    GIc,    GIIc, YTUD, totalthick
   8900.0, 172000.0,   0.35,   4200.0,  0.765,  1.250,41.43,6.0
** thick,      layers,  SLDAT
   0.375,   11.0,   69.40
** X1co, X2co, X6co, X12co,X16co,X26co
   13941.86, 188.53,   38.47,   1328298.33,  292652.05,  4273.75
** X1cc, X2cc, X6cc, X12cc,X16cc,X26cc
   17223.16, 263.45,   39.39,   2268721.84,  339194.44,  5188.41
** X1phy, X2phy, X6phy, X12phy,X16phy,X26phy
   3504.19, 89.82,   27.65,   162337.99,  57786.08,  1377.15
```

Once the output file *jobname.ma* has been generated, the user must change 2 different parts of the .ma file.

1) The name of *jobname.ma* jobname should be the same of the .inp file.

2) In every MAT # X should change the name of the material. This should be written in capital letters and should coincide with the name of the material at the input file. BE CAREFUL in this step!

UVARM subroutine (.for)

The subroutine is attached in Appendix I. Depending on the platform where the analysis is run the extension of the subroutine must be changed:

Windows: MCID_v3.for

Linux: MCID_v3.f

How to run the model

The three files (.inp) (.ma) and (.for) should be at the same directory. The simplest way to run the analysis is from the command window. First access to the directory and then run the following command:

```
abaqus j=example user=MCID.for
```

Post-processing the variables

Once the model has been run the results should be analyzed. As a common ABAQUS result file an example.ODB file will be found in the working space. The result file has to be opened and the UVARM variables will be available for in the menu with the stresses, strains and other output values that have been computed. In the menu three different variables will be found:

UVARM1: Matrix Cracking criterion value from LaRC'03

UVARM2: Delamination onset for generalized plane strain conditions MCID criterion.

UVARM3: Delamination onset for generalized plane stress conditions MCID criterion.

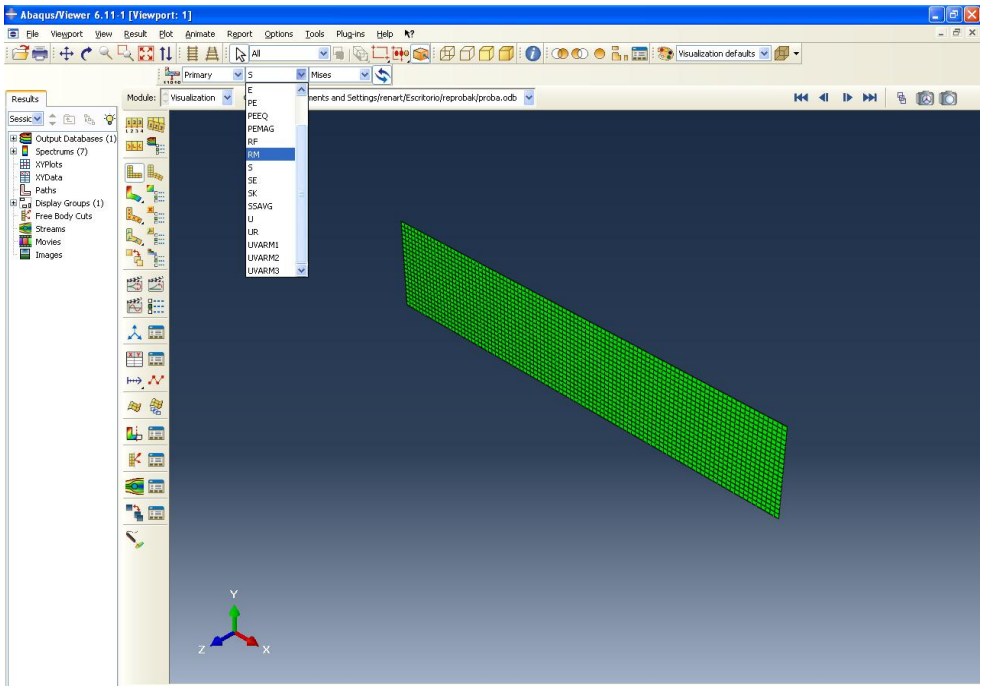

Figure 2 ABAQUS result file view where the result menu with the UVARM variables is shown.

Appendix I: UVARM Subroutine

Delamination onset subrutine: MCID_v3.for

```
C
C
        Module hope
         integer wmatnum, wmatprop(1)
         character(30) wMATNA(200)
         real wMATDATA(15,200)
        end module hope
C
C
        SUBROUTINE UVARM(UVAR,DIRECT,T,TIME,DTIME,CMNAME,ORNAME,
     1 NUVARM,NOEL,NPT,LAYER,KSPT,KSTEP,KINC,NDI,NSHR,COORD,
     2 JMAC,JMATYP,MATLAYO,LACCFLA)
              use hope
C ----------------------------------------------------------------------C
      INCLUDE 'ABA_PARAM.INC'
C ---------------------------------------------------------------------
C     General variables of the subroutine
C
      CHARACTER*80 CMNAME,ORNAME,CMNAME1
      CHARACTER*3 FLGRAY(15)
      CHARACTER xoutdir*255, xfname*80
      CHARACTER dmkname*255, FNAMEX*80
      DIMENSION UVAR(*),DIRECT(3,3),T(3,3),TIME(2)
      DIMENSION ARRAY(15),JARRAY(15),JMAC(*),JMATYP(*),COORD(*)
C
C ---------------------------------------------------------------------
C     Definition of the variables used in the implemented formulation
C
      DIMENSION stress(6)
C
         double precision E22(1),E11(1), nu12(1),G12(1),SMCID12(1),
     &GIc(1),GIIc(1),thick(1),crit(1),del(1), Amat22(1), YisT(1),
     &SisL(1),critmatrix(1),pii(1),YT(1),SL(1),YTUD(1),SLDAT(1),
     &X1MDco(1), X2MDco(1),X6MDco(1), X12MDco(1),ratioY(1),SMCID22(1),
     &critrelation(1),wa(1),wb(1),n(1),X16MDco(1),X26MDco(1),s2(1),
     &X1MDcc(1), X2MDcc(1),X6MDcc(1), X12MDcc(1),X16MDcc(1),X26MDcc(1),
     &X1MDphy(1), X2MDphy(1),X6MDphy(1), X12MDphy(1),X16MDphy(1),
     &X26MDphy(1),del1(1),del2(1)
        Character*80 AAA
        integer precision layers(1),wr
C
C ---------------------------------------------------------------------
C    The nuvarm introduction and uvar variable inizialization
      do i=1,nuvarm
       uvar(i) = 0.d0
      enddo
C Error counter:
      JERROR = 0
C      call uexternaldb
C
C ---------------------------------------------------------------------
C    Recall to Mat_Data which includes the material properties.
C
C
        call getoutdir(xoutdir,lxoutdir)
C
C
        do wr=1,wmatnum
         AAA=wMATNA(wr)
         if(AAA.EQ.CMNAME) then
            E22=wMATDATA(1,wr)
            E11=wMATDATA(2,wr)
```

```
            nu12=wMATDATA(3,wr)
            G12=wMATDATA(4,wr)
            GIc=wMATDATA(5,wr)
            GIIc=wMATDATA(6,wr)
            YTUD=wMATDATA(7,wr)
            totalthick=wMATDATA(8,wr)
            thick=wMATDATA(9,wr)
            layers=wMATDATA(10,wr)
            SLDAT=wMATDATA(11,wr)
            X1MDco=wMATDATA(12,wr)
            X2MDco=wMATDATA(13,wr)
            X6MDco=wMATDATA(14,wr)
            X12MDco=wMATDATA(15,wr)
            X16MDco=wMATDATA(16,wr)
            X26MDco=wMATDATA(17,wr)
            X1MDcc=wMATDATA(18,wr)
            X2MDcc=wMATDATA(19,wr)
            X6MDcc=wMATDATA(20,wr)
            X12MDcc=wMATDATA(21,wr)
            X16MDcc=wMATDATA(22,wr)
            X26MDcc=wMATDATA(23,wr)
            X1MDphy=wMATDATA(24,wr)
            X2MDphy=wMATDATA(25,wr)
            X6MDphy=wMATDATA(26,wr)
            X12MDphy=wMATDATA(27,wr)
            X16MDphy=wMATDATA(28,wr)
            X26MDphy=wMATDATA(29,wr)
          else
          !write(6,*) 'The material has not been found ',CMNAME
          endif
        enddo
C
C
C -------------------------------------------------------------------------
C     Call to the model to obtain the stress values
C
      CALL GETVRM('S',ARRAY,JARRAY,FLGRAY,JRCD,JMAC,JMATYP,MATLAYO,
     &            LACCFLA)
C
       stress(1) = array(1)
       stress(2) = array(2)
       stress(3) = array(3)
       stress(4) = array(4)
       stress(5) = array(5)
       stress(6) = array(6)
C
C -------------------------------------------------------------------------
C     LaRC matrix cracking criterion
C
      pii=3.1416
      critrelation=GIc/GIIc !g at paper
      Amat22= 2.d0*(1.d0/E22-nu12**2.d0/E11)
C     ! If for identifying the outer an inner plies.
       if (LAYER.EQ.1.OR.LAYER.EQ.layers)THEN
        YisT= sqrt(8.d0*GIc/(pii*2.d0*thick*Amat22))
       else
         YisT= sqrt(8.d0*GIc/(pii*thick*Amat22))
      endif
C     For thick plies
      YT=1.12*YTUD*sqrt(2.d0)
      ratioY=YisT/YT
      if (ratioY(1).GT.1.d0) then
           YisT=YisT
      else
       YisT=YT
      endif
C
C     Resume expressions for Sil for thin plies
C
       if (LAYER.EQ.1.OR.LAYER.EQ.layers)THEN
        SisL=sqrt(4.d0*G12*GIIc/pii/thick)
       else
```

```
     SisL=sqrt(8.d0*G12*GIIc/pii/thick)
      endif
C     For thick plies
      SL=SLDAT*sqrt(2.d0)
      if (SisL(1).GT.SL(1)) then
           SisL=SisL
      else
       SisL=SL
      endif
C
C
      critmatrix=(1.d0-critrelation)*stress(2)/YisT+
     &critrelation*(stress(2)/YisT)**2.d0+
     &(stress(4)/SisL)**2.d0
      uvar(1)=critmatrix(1)
C
C ---------------------------------------------------------------------
C     Delamination onset criterion
C     Delamination onset criterion
      if (stress(2).GT.0.0) then !Condition if s2 compression no work
        s2=stress(2)
C        del1=X1MDco
      del1= (stress(1)/X1MDco)*(stress(1)/X1MDco)+(s2/X2MDco)*
     &(s2/X2MDco)+(stress(4)/X6MDco)*(stress(4)/X6MDco)+
     &stress(1)*s2/X12MDco+stress(1)*stress(4)/X16MDco+
     &s2*stress(4)/X26MDco
      else
C      del1=stress(2)*stress(2)
        s2=0
        del1= (stress(1)/X1MDcc)*(stress(1)/X1MDcc)+(s2/X2MDcc)*
     &(s2/X2MDcc)+(stress(4)/X6MDcc)*(stress(4)/X6MDcc)+
     &stress(1)*s2/X12MDcc+stress(1)*stress(4)/X16MDcc+
     &s2*stress(4)/X26MDcc
      endif

C      del2=stress(1)*stress(1)
C
      del2=(stress(1)/X1MDphy)*(stress(1)/X1MDphy)+(stress(2)/X2MDphy)*
     &(stress(2)/X2MDphy)+(stress(4)/X6MDphy)*(stress(4)/X6MDphy)+
     &stress(1)*s2/X12MDphy+stress(1)*stress(4)/X16MDphy+
     &s2*stress(4)/X26MDphy
C
C ---------------------------------------------------------------------
C     Output variables
C
      uvar(2)=del1(1)
      uvar(3)=del2(1)
C      uvar(3)=SMCID22(1)
C      uvar(4)=SMCID12(1)
C      uvar(5)=YisT(1)
C      uvar(6)=SisL(1)
C
C
C
C If error, write comment to .DAT file:
      IF(JERROR.NE.0)THEN
        WRITE(6,*) 'REQUEST ERROR IN UVARM FOR ELEMENT NUMBER ',
     1      NOEL,'INTEGRATION POINT NUMBER ',NPT
      ENDIF
      RETURN
      END
C
C
* <<<<<<<<<<<<<<<<<<<<<<<< FUNCTION DMKNAME  >>>>>>>>>>>>>>>>>>>>>>>> *
*                                                                     *
*               Compose a filename directory/jobname.exten            *
*                                                                     *
* <<<<<<<<<<<<<<<<<<<<<<<<<<<<<<<<<<<<<<<<<<<<<<<<<<<<<<<<<<<<<<<<<< *
      character*(*) function dmkname(fname,dname,exten)
C
      character*(*) fname,dname,exten
C
```

```
C
      ltot = len(fname)
      lf = 0
      do k1 = ltot,2,-1
        if (lf.eq.0.and.fname(k1:k1).ne.' ')  lf = k1
      end do
C
      ltot = len(dname)
      ld = 0
      do k1 = ltot,2,-1
        if (ld.eq.0.and.dname(k1:k1).ne.' ')  ld = k1
      end do
C
      ltot = len(exten)
      le = 0
      do k1 = ltot,2,-1
        if (le.eq.0.and.exten(k1:k1).ne.' ')  le = k1
      end do
C
      if ((lf + ld + le) .le. len(dmkname)) then
        dmkname = dname(1:ld)//'/'//fname(1:lf)
        ltot = ld + lf + 1
        if ( le.gt.0) then
           dmkname = dmkname(1:ltot)//exten(1:le)
        end if
      end if
C
      return
      end
*<<<<<<<<<<<<<<<<<<<<<<<<<SUBROUTINE UEXTERNALDB<<<<<<<<<<<<<<<<<<<<<<<<*
*                                                                         *
*         SUBROUTINE TO BE CALLED AT THE END OF EACH INCREMENT            *
*                                                                         *
*<<<<<<<<<<<<<<<<<<<<<<<<<<<<<<<<<<<<<<<<<<<<<<<<<<<<<<<<<<<<<<<<<<<<<<<*
C
      subroutine uexternaldb(lop,lrestart,time,dtime,kstep,kinc)
C
         use hope
        INCLUDE 'ABA_PARAM.INC'
C
        CHARACTER xindir*255, xfname*80
        CHARACTER dmkname*255, FNAMEX*80
        CHARACTER wa0*30
C
        real wa1, wa2,wa3,wa4,wa5,wa6,
     &wa7,wa8,wa9,wa10,wa11,wa12,wa13,wa14,
     &wa15,wa16,wa17,wa18,wa19,wa20,wa21,
     &wa22,wa23,wa24,wa25,wa26,wa27,wa28,wa29
C
C
C
       wmat_num=1
       wmat_prop=1
C
C AT THE START OF THE ANALYSIS
        IF (LOP.EQ.0) THEN
          lxfname = 0
          lxindir = 0
          xfname  =' '
          xindir  =' '
C      open files
          call getjobname(xfname,lxfname)     !input file name
          call getoutdir(xindir,lxindir)    !input directory
          FNAMEX=dmkname(xfname(1:lxfname),xindir(1:lxindir),'.ma')
          open(unit=17,file=FNAMEX)
C      initialize "common" variables
C
C
C
       read (17,*) wmatnum
       do r=1, wmatnum
       read (17,*)
```

```
          read (17,*) wa0
    C
    C     Once the material properties file is found the material properties
    C  are read and the variables are saved.
    C
            read (17,*) !Properties descrip line1 at .ma
            read (17,*) wa1, wa2, wa3, wa4, wa5, wa6, wa7,wa8
            read (17,*) !Properties descrip line 2 at .ma
            read (17,*) wa9,wa10,wa11
            read (17,*) !Properties descrip line 3 at .ma
            read (17,*) wa12,wa13,wa14,wa15,wa16,wa17
            read (17,*) !Properties descrip line 4 at .ma
            read (17,*) wa18,wa19,wa20,wa21,wa22,wa23
            read (17,*) !Properties descrip line 5 at .ma
            read (17,*) wa24,wa25,wa26,wa27,wa28,wa29
    C
             wMATNA(r)=wa0
    C
            wMATDATA(1,r)=wa1
            wMATDATA(2,r)=wa2
            wMATDATA(3,r)=wa3
            wMATDATA(4,r)=wa4
            wMATDATA(5,r)=wa5
            wMATDATA(6,r)=wa6
            wMATDATA(7,r)=wa7
            wMATDATA(8,r)=wa8
            wMATDATA(9,r)=wa9
            wMATDATA(10,r)=wa10
            wMATDATA(11,r)=wa11
            wMATDATA(12,r)=wa12
            wMATDATA(13,r)=wa13
            wMATDATA(14,r)=wa14
            wMATDATA(15,r)=wa15
            wMATDATA(16,r)=wa16
            wMATDATA(17,r)=wa17
            wMATDATA(18,r)=wa18
            wMATDATA(19,r)=wa19
            wMATDATA(20,r)=wa20
            wMATDATA(21,r)=wa21
            wMATDATA(22,r)=wa22
            wMATDATA(23,r)=wa23
            wMATDATA(24,r)=wa24
            wMATDATA(25,r)=wa25
            wMATDATA(26,r)=wa26
            wMATDATA(27,r)=wa27
            wMATDATA(28,r)=wa28
            wMATDATA(29,r)=wa29
          enddo
    C
            ENDIF
    C AT THE START OF THE CURRENT ANALYSIS INCREMENT (REPEATED INCREMENT FAILS AND
PNWEDT)
            IF (LOP.EQ.1) THEN
            ENDIF
    C AT THE END OF THE CURRENT (CONVERGED) ANALYSIS INCREMENT
            IF (LOP.EQ.2) THEN
            ENDIF
    C AT THE END OF THE ANALYSIS
            IF (LOP.EQ.3) THEN
              write(6,*) 'The materials are ',wMATNA
              WRITE(16,*)"END OF THE SUBROUTINE",KSTEP,KINC
              WRITE(15,*)"END OF THE SUBROUTINE",KSTEP,KINC
              CLOSE(unit=15)
              CLOSE(unit=16)
            ENDIF
    C
            RETURN
          END
    *=================================================================*
    *=================================================================*
    *                                                                 *
    *                       END OF PROGRAM                            *
```

```
*                                                                     *
*=====================================================================*
*=====================================================================*
```

Appendix II: MATLAB file to generate .ma files.

Matlab file:

```
%
% .ma generation file for subroutine
%
% L.Zubillaga, A.Turon.

clear all,close all, clc;

clear all,close all, clc;

% Transversely isotropic material need 4 constants:
% E1, E2, nu12, G12 YTUD, SLDAT(MPa) GIc GIIc ()
Mat(1,:)=[172000, 8900, 0.35, 4200, 41.43, 69.4, .765, 1.25]; %CAR_EPO
%%
%Measurement of the material matrix
[n_mat,n_prop]=size(Mat);

% The lamina need to define material, angle and thickness
L(1,:)=[1, 30, 0.25];
L(2,:)=[1, -30, 0.25];
L(3,:)=[1, 90, 0.5];
L(4,:)=[1, 30, 0.25];
L(5,:)=[1, -30, 0.25];
L(6,:)=[1, 90,1.0];
L(7,:)=[1, -30, 0.25];
L(8,:)=[1, 30, 0.25];
L(9,:)=[1, 90, 0.5];
L(10,:)=[1, -30, 0.25];
L(11,:)=[1, 30, 0.25];

% L(1,:)=[1, 45, 0.5625];
% L(2,:)=[1, -45, 0.375];
% L(3,:)=[1, 45, 0.5625];

%Reduction factor definition for damaged plies
rev=0.0001;

%Number of laminas at the laminate.
n_lam=size(L,1);

% Computation of the half ply for symmetrical laminates
aaaa=fix(n_lam/2);
bbbb=rem(n_lam,2);
if bbbb==0
    MM=aaaa;
else
MM=aaaa+1;
end
```

```
% n_lamMM=size(MM,1)

for y=1:MM%n_lamMM
    %r=MM(y);
    %Angle obtation for each ply
    theta=L(y,2);

    %Rotation of the laminate to obtain the local axis of the studied
    %lamina
        for j=1:n_lam
            L1(j,:)=L(j,:)-[0, theta, 0]; %local axis orientation
        end


            % Compute S and Q
            for g=1:n_lam;
                i_mat=L1(g,1); %material type
                S(1,1,g)=1/Mat(i_mat,1);
                S(1,2,g)=-Mat(i_mat,3)/Mat(i_mat,1);
                S(2,1,g)=S(1,2,g);
                S(2,2,g)=1/Mat(i_mat,2);
                S(3,3,g)=1/Mat(i_mat,4);

                Q(:,:,g)=inv(S(:,:,g));
            end;

            % Compute transformation matrices T and Tgamma (in LOCAL
axis)
            for is=1:n_lam;
                theta=L1(is,2)*pi/180;

                m=cos(theta);
                n=sin(theta);

                T(1,1,is)=m^2;
                T(1,2,is)=n^2;
                T(1,3,is)=2*m*n;
                T(2,1,is)=n^2;
                T(2,2,is)=m^2;
                T(2,3,is)=-2*m*n;
                T(3,1,is)=-m*n;
                T(3,2,is)=m*n;
                T(3,3,is)=m^2-n^2;

                Tg(:,:,is)=(inv(T(:,:,is)))';

            % Compute stiffness and compliance transformed matrices
                Sb(:,:,is)=inv(Tg(:,:,is))*S(:,:,is)*T(:,:,is);
                Qb(:,:,is)=inv(Sb(:,:,is));
            end;

            % Laminate constitutive matrix (ABD)
            % Location of the bounds of the laminae and laminate's
midplane
            TH=0;
```

```
            Z=zeros(n_lam+1,1);
            for i=1:n_lam;
                TH=TH+L(i,3);
            end;
            th=TH/2;
            TH=0;
            Z(1)=-th;
            for i=1:n_lam;
                TH=TH+L(i,3);
                Z(i+1)=TH-th;
            end;

            % Compute A matrix
            A=zeros(3,3);
            for i=1:n_lam;
                for j=1:3;
                    for k=1:3;
                        A(j,k)=A(j,k)+Qb(j,k,i)*(Z(i+1)-Z(i));
                    end;
                end;
            end;
            % Compute B matrix
            B=zeros(3,3);
            for i=1:n_lam;
                for j=1:3;
                    for k=1:3;
                        B(j,k)=B(j,k)+Qb(j,k,i)*(Z(i+1)^2-
Z(i)^2)*(1/2);
                    end;
                end;
            end;

            % Compute D matrix
            D=zeros(3,3);
            for i=1:n_lam;
                for j=1:3;
                    for k=1:3;
                        D(j,k)=D(j,k)+Qb(j,k,i)*(Z(i+1)^3-
Z(i)^3)*(1/3);
                    end;
                end;
            end;
            ABD=zeros(6,6);
            ABD=[A B; B D];


            % Compute S and Q
            %Crack opening=co
            for g1=1:n_lam;
                if g1==y
                    i_mat=L1(g1,1);
                    S1(1,1,g1)=1/Mat(i_mat,1);
                    S1(1,2,g1)=Mat(i_mat,3)*rev/Mat(i_mat,1);
                    S1(2,1,g1)=S1(1,2,g1);
                    S1(2,2,g1)=1/Mat(i_mat,2)/rev;
                    S1(3,3,g1)=1/Mat(i_mat,4)/rev;
```

```
                    Q1(:,:,g1)=inv(S1(:,:,g1));
                else

                    i_mat=L1(g1,1);
                    S1(1,1,g1)=1/Mat(i_mat,1);
                    S1(1,2,g1)=-Mat(i_mat,3)/Mat(i_mat,1);
                    S1(2,1,g1)=S1(1,2,g1);
                    S1(2,2,g1)=1/Mat(i_mat,2);
                    S1(3,3,g1)=1/Mat(i_mat,4);

                    Q1(:,:,g1)=inv(S1(:,:,g1));
                end;

            end


            % Compute stiffness and compliance transformed matrices
            for is=1:n_lam;
                Sb1(:,:,is)=inv(Tg(:,:,is))*S1(:,:,is)*T(:,:,is);
                Qb1(:,:,is)=inv(Sb1(:,:,is));
            end;


            Aco=zeros(3,3);
            for u=1:n_lam
               for j=1:3;
                    for k=1:3;
                        Aco(j,k)=Aco(j,k)+Qb1(j,k,u)*(Z(u+1)-Z(u));
                    end;
               end;
           end;
                        % Compute B matrix
            Bco=zeros(3,3);
            for u=1:n_lam;
                for j=1:3;
                    for k=1:3;
                        Bco(j,k)=Bco(j,k)+Qb1(j,k,u)*(Z(u+1)^2-
Z(u)^2)*(1/2);
                    end;
                end;
            end;

            % Compute D matrix
            Dco=zeros(3,3);
            for u=1:n_lam;
                for j=1:3;
                    for k=1:3;
                        Dco(j,k)=Dco(j,k)+Qb1(j,k,u)*(Z(u+1)^3-
Z(u)^3)*(1/3);
                    end;
                end;
            end;
            ABDco=zeros(6,6);
            ABDco=[Aco Bco; Bco Dco];
```

```
            %Crack closing=cc
            for g2=1:n_lam;
                if g2==y
                    i_mat=L1(g2,1);
                    S2(1,1,g2)=1/Mat(i_mat,1);
                    S2(1,2,g2)=-Mat(i_mat,3)/Mat(i_mat,1);
                    S2(2,1,g2)=S2(1,2,g2);
                    S2(2,2,g2)=1/Mat(i_mat,2);
                    S2(3,3,g2)=1/Mat(i_mat,4)/rev;

                    Q2(:,:,g2)=inv(S2(:,:,g2));
                else

                    i_mat=L1(g2,1);
                    S2(1,1,g2)=1/Mat(i_mat,1);
                    S2(1,2,g2)=-Mat(i_mat,3)/Mat(i_mat,1);
                    S2(2,1,g2)=S2(1,2,g2);
                    S2(2,2,g2)=1/Mat(i_mat,2);
                    S2(3,3,g2)=1/Mat(i_mat,4);

                    Q2(:,:,g2)=inv(S2(:,:,g2));
                end;

            end

            % Compute stiffness and compliance transformed matrices
            for is=1:n_lam;
                Sb2(:,:,is)=inv(Tg(:,:,is))*S2(:,:,is)*T(:,:,is);
                Qb2(:,:,is)=inv(Sb2(:,:,is));
            end;


            Acc=zeros(3,3);
            for u=1:n_lam
               for j=1:3;
                    for k=1:3;
                        Acc(j,k)=Acc(j,k)+Qb2(j,k,u)*(Z(u+1)-Z(u));
                    end;
               end;
           end;
                        % Compute B matrix
            Bcc=zeros(3,3);
            for u=1:n_lam;
                for j=1:3;
                    for k=1:3;
                        Bcc(j,k)=Bcc(j,k)+Qb2(j,k,u)*(Z(u+1)^2-
Z(u)^2)*(1/2);
                    end;
                end;
            end;

            % Compute D matrix
            Dcc=zeros(3,3);
```

```
            for u=1:n_lam;
                for j=1:3;
                    for k=1:3;
                        Dcc(j,k)=Dcc(j,k)+Qb2(j,k,u)*(Z(u+1)^3-
Z(u)^3)*(1/3);
                    end;
                end;
            end;
            ABDcc=zeros(6,6);
            ABDcc=[Acc Bcc; Bcc Dcc];

                                % Compute S and Q
            %Angle not 0°=phy
            for g3=1:n_lam;
                if g3==y
                    i_mat=L1(g3,1);
                    S3(1,1,g3)=1/Mat(i_mat,1)/rev;
                    S3(1,2,g3)=-Mat(i_mat,3)*rev/Mat(i_mat,1)/rev;
                    S3(2,1,g3)=S3(1,2,g3);
                    S3(2,2,g3)=1/Mat(i_mat,2)/rev;
                    S3(3,3,g3)=1/Mat(i_mat,4)/rev;

                    Q3(:,:,g3)=inv(S3(:,:,g3));
                else

                    i_mat=L1(g3,1);
                    S3(1,1,g3)=1/Mat(i_mat,1);
                    S3(1,2,g3)=-Mat(i_mat,3)/Mat(i_mat,1);
                    S3(2,1,g3)=S3(1,2,g3);
                    S3(2,2,g3)=1/Mat(i_mat,2);
                    S3(3,3,g3)=1/Mat(i_mat,4);

                    Q3(:,:,g3)=inv(S3(:,:,g3));
                end;

            end

            % Compute stiffness and compliance transformed matrices
            for is=1:n_lam;
                Sb3(:,:,is)=inv(Tg(:,:,is))*S3(:,:,is)*T(:,:,is);
                Qb3(:,:,is)=inv(Sb3(:,:,is));
            end;


            Aphy=zeros(3,3);
            for u=1:n_lam
               for j=1:3;
                    for k=1:3;
                        Aphy(j,k)=Aphy(j,k)+Qb3(j,k,u)*(Z(u+1)-Z(u));
                    end;
               end;
           end;
                        % Compute B matrix
            Bphy=zeros(3,3);
            for u=1:n_lam;
                for j=1:3;
```

```
                    for k=1:3;
                        Bphy(j,k)=Bphy(j,k)+Qb3(j,k,u)*(Z(u+1)^2-
Z(u)^2)*(1/2);
                    end;
                end;
            end;

            % Compute D matrix
            Dphy=zeros(3,3);
            for u=1:n_lam;
                for j=1:3;
                    for k=1:3;
                        Dphy(j,k)=Dphy(j,k)+Qb3(j,k,u)*(Z(u+1)^3-
Z(u)^3)*(1/3);
                    end;
                end;
            end;
            ABDphy=zeros(6,6);
            ABDphy=[Aphy Bphy; Bphy Dphy];



           %%
           nn=0;
           if y==1
               nn=1;
           else
               nn=2;
           end

            ABDbarco=zeros(6,6);
            ABDbarco=inv(ABDco)-inv(ABD);
            abarco=zeros(3,3);
            abarco=ABDbarco(1:3,1:3);
            chico=zeros(3,3);
            chico=abs(S(:,:,y)'*A'*abarco*A*S(:,:,y));
            X1co=sqrt((2*nn*Mat(i_mat,8))/chico(1,1));
            X2co=sqrt((2*nn*Mat(i_mat,8))/chico(2,2));
            X6co=sqrt((2*nn*Mat(i_mat,8))/chico(3,3));
            X12co=(2*nn*Mat(i_mat,8))/(chico(1,2)+chico(2,1));
            X16co=(2*nn*Mat(i_mat,8))/(chico(1,3)+chico(3,1));
            X26co=(2*nn*Mat(i_mat,8))/(chico(2,3)+chico(3,2));
            %%
            ABDbarcc=zeros(6,6);
            ABDbarcc=inv(ABDcc)-inv(ABD);
            abarcc=zeros(3,3);
            abarcc=ABDbarcc(1:3,1:3);
            chicc=zeros(3,3);
            chicc=abs(S(:,:,y)'*A'*abarcc*A*S(:,:,y));
            X1cc=sqrt((2*nn*Mat(i_mat,8))/chicc(1,1));
            X2cc=sqrt((2*nn*Mat(i_mat,8))/chicc(2,2));
            X6cc=sqrt((2*nn*Mat(i_mat,8))/chicc(3,3));
            X12cc=(2*nn*Mat(i_mat,8))/(chicc(1,2)+chicc(2,1));
            X16cc=(2*nn*Mat(i_mat,8))/(chicc(1,3)+chicc(3,1));
            X26cc=(2*nn*Mat(i_mat,8))/(chicc(2,3)+chicc(3,2));
            %%
```

```
            ABDbarphy=zeros(6,6);
            ABDbarphy=inv(ABDphy)-inv(ABD);
            abarphy=zeros(3,3);
            abarphy=ABDbarphy(1:3,1:3);
            chiphy=zeros(3,3);
            chiphy=abs(S(:,:,y)'*A'*abarphy*A*S(:,:,y));
            X1phy=sqrt((2*nn*Mat(i_mat,8))/chiphy(1,1));
            X2phy=sqrt((2*nn*Mat(i_mat,8))/chiphy(2,2));
            X6phy=sqrt((2*nn*Mat(i_mat,8))/chiphy(3,3));
            X12phy=(2*nn*Mat(i_mat,8))/(chiphy(1,2)+chiphy(2,1));
            X16phy=(2*nn*Mat(i_mat,8))/(chiphy(1,3)+chiphy(3,1));
            X26phy=(2*nn*Mat(i_mat,8))/(chiphy(2,3)+chiphy(3,2));

            ty=L(y,1);
            result(y,:)=[Mat(ty,2),Mat(ty,1), Mat(ty,3), Mat(ty, 4),
Mat(ty,7), Mat(ty,8), Mat(ty,5),L(y,3),n_lam,  Mat(ty, 6),X1co, X2co,
X6co, X12co,X16co,X26co,X1cc, X2cc, X6cc, X12cc,X16cc,X26cc,X1phy,
X2phy, X6phy, X12phy,X16phy,X26phy];
end




%%%%%%%%%%%%%%%%%%%%%%%%%%%%   CREATE .mt FILE
%%%%%%%%%%%%%%%%%%%%%%%%%%%%
fid = fopen('jobname.ma','w');
fprintf(fid,'\n %1.0f',MM );
for i=1:MM
 fprintf(fid,'\n** MAT. #%1.0f',i );
 fprintf(fid,': MATERIAL NAME: Description of the material ');
 fprintf(fid,'\n   MATERIAL NAME IN CAPS');
 fprintf(fid,'\n** E22,       E11,       nu12 ,      G21,    GIc,
GIIc, YTUD');
 fprintf(fid,'\n   %1.1f, %1.1f,   %1.2f,   %1.1f,  %1.3f,
%1.3f,%1.2f',...
     result(i,1), result(i,2), result(i,3), result(i,4), result(i,5),
result(i,6), result(i,7));
 fprintf(fid,'\n** thick,      layers,  SLDAT');
 fprintf(fid,'\n   %1.3f,   %1.1f,   %1.2f',...
    result(i,8), result(i,9), result(i,10));
 fprintf(fid,'\n** X1co, X2co, X6co, X12co,X16co,X26co');
 fprintf(fid,'\n   %1.2f, %1.2f,   %1.2f,   %1.2f,  %1.2f,  %1.2f',...
     result(i,11), result(i,12), result(i,13), result(i,14),
result(i,15), result(i,16));
 fprintf(fid,'\n** X1cc, X2cc, X6cc, X12cc,X16cc,X26cc');
 fprintf(fid,'\n   %1.2f, %1.2f,   %1.2f,   %1.2f,  %1.2f,  %1.2f',...
     result(i,17), result(i,18), result(i,19), result(i,20),
result(i,21), result(i,22));
 fprintf(fid,'\n** X1phy, X2phy, X6phy, X12phy,X16phy,X26phy');
 fprintf(fid,'\n   %1.2f, %1.2f,   %1.2f,   %1.2f,  %1.2f,  %1.2f',...
     result(i,23), result(i,24), result(i,25), result(i,26),
result(i,27), result(i,28));
end
fclose(fid);
```

Appendix III: Examples

Example I: Definition of material in the .inp and .ma

It is an important fact to take into account while generating the .inp file the nomenclature of the material for the laminate. Material definition should be different for every ply that has a different material and/or orientation and/or ply thickness. For the laminate definition in the .inp file.

```
*Shell Section, elset=SHELL, composite, orient=or0

    0.25, 3, CAR-EPO, 30.
    0.25, 3, CAR-EPO, -30.
    0.5, 3, CAR-EPO, 90.
    0.25, 5, CAR-EPO, 30.
    0.25, 3, CAR-EPO, -30.
    1.0, 3, CAR-EPO, 90.
    0.25, 3, CAR-EPO, -30.
    0.25, 5, CAR-EPO, 30.
    0.5, 3, CAR-EPO, 90.
    0.25, 3, CAR-EPO, -30.
    0.25, 3, CAR-EPO, 30.
```

a matlab file containing the information should be defined. Which will determine different material types.

```
% The lamina need to define material, angle and thickness

L(1,:)=[1, 30, 0.25];  --> Material 1
L(2,:)=[1, -30, 0.25]; --> Material 2;
L(3,:)=[1, 90, 0.5];   --> Material 3;
L(4,:)=[1, 30, 0.25];  --> Material 1;
L(5,:)=[1, -30, 0.25]; --> Material 2;
L(6,:)=[1, 90,1.0];    --> Material 4;
L(7,:)=[1, -30, 0.25]; --> Material 2; Identical to ply 5
L(8,:)=[1, 30, 0.25];  --> Material 1; Identical to ply 4
L(9,:)=[1, 90, 0.5];   --> Material 3; Identical to ply 3
L(10,:)=[1, -30, 0.25];--> Material 2; Identical to ply 2
L(11,:)=[1, 30, 0.25]; --> Material 1; Identical to ply 1
```

And will generate .ma file containing the different properties for each type.

```
6
** MAT. #1: MATERIAL NAME: Description of the material
   MATERIAL NAME IN CAPS
** E22,       E11,       nu12 ,      G21,    GIc,    GIIc, YTUD
   8900.0, 172000.0,   0.35,   4200.0,  0.765,  1.250,41.43
** thick,      layers,  SLDAT
   0.250,   11.0,   69.40
** X1co, X2co, X6co, X12co,X16co,X26co
   1647110.45, 294.68,   200.57,   23828526892.31,  4348227243372.71,  7784793.78
** X1cc, X2cc, X6cc, X12cc,X16cc,X26cc
   43959920484.22, 2226827008.22,   200.57,   117170491197781590000.00,
320169412299721210000.00,  5303794935849020400.00
** X1phy, X2phy, X6phy, X12phy,X16phy,X26phy
   837.00, 292.67,   200.57,   1051189.04,  95399879.45,  8002396.71
```

```
   ** MAT. #2: MATERIAL NAME: Description of the material
      MATERIAL NAME IN CAPS
   ** E22,       E11,       nu12 ,      G21,    GIc,    GIIc, YTUD
      8900.0, 172000.0,   0.35,   4200.0,  0.765,  1.250,41.43
   ** thick,      layers,  SLDAT
      0.250,   11.0,   69.40
   ** X1co, X2co, X6co, X12co,X16co,X26co
      2329364.96, 418.46,   285.26,   48049483251.74,  43863872050490.43,  78002730.26
   ** X1cc, X2cc, X6cc, X12cc,X16cc,X26cc
      71615064334.38, 4011905897.16,   285.26,   341137272932323890000.00,
698352195929375510000.00,  36504249584194707000.00
   ** X1phy, X2phy, X6phy, X12phy,X16phy,X26phy
      1179.76, 415.57,   285.26,   2090067.68,  604933406.28,  81502153.96
   ** MAT. #3: MATERIAL NAME: Description of the material
      MATERIAL NAME IN CAPS
   ** E22,       E11,       nu12 ,      G21,    GIc,    GIIc, YTUD
      8900.0, 172000.0,   0.35,   4200.0,  0.765,  1.250,41.43
   ** thick,      layers,  SLDAT
      0.500,   11.0,   69.40
   ** X1co, X2co, X6co, X12co,X16co,X26co
      1647111.17, 293.47,   199.45,   23636116076.15,  4949162286276.20,  8873723.11
   ** X1cc, X2cc, X6cc, X12cc,X16cc,X26cc
      20717768081643622000.00, 208542652434061180.00,   199.45,
19626845610309452000000000000000000000.00,  5445207898415767200000.00,
280187480339919960000.00
   ** X1phy, X2phy, X6phy, X12phy,X16phy,X26phy
      768.42, 291.15,   199.45,   889945.79,  104202279.73,  9131664.46
```

The user should introduce the name for each material in the .ma file and should be coincident with the ones at the .inp

For example:

```
*Shell Section, elset=SHELL, composite, orient=or0



0.25, 3, CAR-EPO-1, 30.
0.25, 3, CAR-EPO-2, -30.
0.5, 3, CAR-EPO-3, 90.
0.25, 5, CAR-EPO-4, 30.
0.25, 3, CAR-EPO-5, -30.
1.0, 3, CAR-EPO-6, 90.
0.25, 3, CAR-EPO-5, -30.
0.25, 5, CAR-EPO-4, 30.
0.5, 3, CAR-EPO-3, 90.
0.25, 3, CAR-EPO-2, -30.
0.25, 3, CAR-EPO-1, 30.
```

and

```
   ** MAT. #1: MATERIAL NAME: Description of the material
      CAR-EPO-1
   ** E22,       E11,       nu12 ,      G21,    GIc,    GIIc, YTUD
      8900.0, 172000.0,   0.35,   4200.0,  0.765,  1.250,41.43
   ** thick,      layers,  SLDAT
      0.250,   11.0,   69.40
   ** X1co, X2co, X6co, X12co,X16co,X26co
      1647110.45, 294.68,   200.57,   23828526892.31,  4348227243372.71,  7784793.78
   ** X1cc, X2cc, X6cc, X12cc,X16cc,X26cc
      43959920484.22, 2226827008.22,   200.57,   117170491197781590000.00,
320169412299721210000.00,  5303794935849020400.00
   ** X1phy, X2phy, X6phy, X12phy,X16phy,X26phy
      837.00, 292.67,   200.57,   1051189.04,  95399879.45,  8002396.71
   ** MAT. #2: MATERIAL NAME: Description of the material
      CAR-EPO-2
```

```
   ** E22,       E11,       nu12 ,      G21,    GIc,    GIIc, YTUD
      8900.0, 172000.0,   0.35,   4200.0,  0.765,  1.250,41.43
   ** thick,      layers,  SLDAT
      0.250,   11.0,   69.40
   ** X1co, X2co, X6co, X12co,X16co,X26co
      2329364.96, 418.46,   285.26,   48049483251.74,  43863872050490.43,  78002730.26
   ** X1cc, X2cc, X6cc, X12cc,X16cc,X26cc
      71615064334.38, 4011905897.16,   285.26,   341137272932323890000.00,
6983521959293755100000.00,  365042495841947070000.00
   ** X1phy, X2phy, X6phy, X12phy,X16phy,X26phy
      1179.76, 415.57,   285.26,   2090067.68,  604933406.28,  81502153.96
```

Example II: full .inp and .ma files

The proposed model has the next characteristics:

Lay up: $(30_2/-30_2/90_4/30_2/-30_2/90_4)_s$

Material properties: Carbon-Epoxy:

E_{11}=172 GPa

E_{22}=8.9 GPa

υ_{12}=0.35

G_{12}=4.2GPa

Y_T^{UD}=41.43 MPa

S_L^{DAT}=69.40 MPa

G_{Ic}= 0.765 N/mm

G_{IIc}= 1.25 N/mm

Specimens: a rectangular specimen has been tested 20X100X4 (mm)(WXLXt)

The loading conditions for the specimen shown:Figure 3.

One side of the width: fixed in direction 1, 2 (in plane)

Opposite side of the width: Displacement in direction 1,2 of 2.0mm.in 20 substeps.

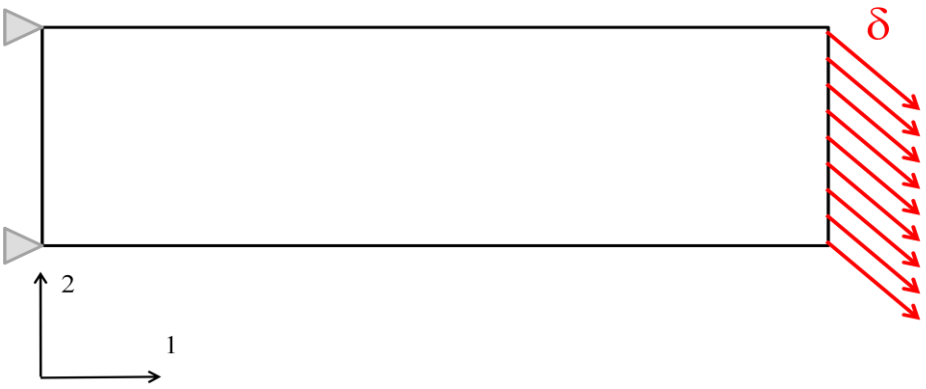

Figure 3 MCID_v2Example's schematic representation

MCID_v3Example.inp file

```
*HEADING
 MCID_v2.for Example
**PREPRINT, MODEL=YES, ECHO=YES, HISTORY=YES
**
**********************************************************************
***                          INPUT PARAMETERS                      ***
**********************************************************************
*PARAMETER
** Properties of the specimen interface:
**
** Applied displacement (mm):
** Step-1
 disp_1 = 2.0
 inc1 = 0.10
**
t1 = disp_1
**
**
**********************************************************************
**             GENERATION OF NODES AND NSETS                    **
**********************************************************************
*NODE
      1,      0.,   0.
     100,  100.,   0.
  2001,      0.,  20.
  2100,  100.,  20.
**
*NGEN, NSET=L1
    1,       100, 1
 *NGEN, NSET=L2
 2001,   2100, 1
**
*NFILL, NSET=S1
 L1,L2, 20,100
**
**
*NSET, NSET=nleft
     1,101,201,301,401,501,601,701,801,901
     1001,1101,1201,1301,1401,1501,1601,1701,1801,1901,2001
*NSET, NSET=nright
     100,200,300,400,500,600,700,800,900,1000
     1100,1200,1300,1400,1500,1600,1700,1800,1900,2000,2100
**
**********************************************************************
**          DEFINE ELEMENTS & LAMINATE PROPERTIES               **
**********************************************************************
*ELEMENT, TYPE=S4
      1,      1,     2,   102,   101,
**
*ELGEN, ELSET=SHELL
      1, 99, 1, 1, 20, 100, 100
**
*ORIENTATION, NAME=or0
 1.0, 0.0, 0.0, 0.0, 1.0, 0.0
 3, 0
*ORIENTATION,NAME=or10
 1.0, 0.0, 0.0, 0.0, 1.0, 0.0
 3, 10
**
*Shell Section, elset=SHELL, composite, orient=or0
0.25, 3, CAR-EPO-1, 30.
0.25, 3, CAR-EPO-2, -30.
0.5, 3, CAR-EPO-3, 90.
0.25, 5, CAR-EPO-4, 30.
0.25, 3, CAR-EPO-5, -30.
1.0, 3, CAR-EPO-6, 90.
0.25, 3, CAR-EPO-5, -30.
0.25, 5, CAR-EPO-4, 30.
0.5, 3, CAR-EPO-3, 90.
```

```
0.25, 3, CAR-EPO-2, -30.
0.25, 3, CAR-EPO-1, 30.
**
*Material, name= CAR-EPO-1
*Elastic, type=LAMINA
172000.,8900., 0.35,4200.,4200.,2908.
*USER OUTPUT VARIABLES
 3,
**
*Material, name= CAR-EPO-2
*Elastic, type=LAMINA
172000.,8900., 0.35,4200.,4200.,2908.
*USER OUTPUT VARIABLES
 3,
**
*Material, name= CAR-EPO-3
*Elastic, type=LAMINA
172000.,8900., 0.35,4200.,4200.,2908.
*USER OUTPUT VARIABLES
 3,
**
*Material, name= CAR-EPO-4
*Elastic, type=LAMINA
172000.,8900., 0.35,4200.,4200.,2908.
*USER OUTPUT VARIABLES
 3,
*Material, name= CAR-EPO-5
*Elastic, type=LAMINA
172000.,8900., 0.35,4200.,4200.,2908.
*USER OUTPUT VARIABLES
 3,
*Material, name= CAR-EPO-6
*Elastic, type=LAMINA
172000.,8900., 0.35,4200.,4200.,2908.
*USER OUTPUT VARIABLES
 3,

**
**
**********************************************************************
***                        BOUNDARY CONDITIONS                       ***
**********************************************************************
**
*BOUNDARY,TYPE=DISPLACEMENT
 nleft,1,2
 1,3,3
**
**********************************************************************
***                        INITIAL CONDITIONS                        ***
**********************************************************************
**
**
**
**********************************************************************
***                             DEFINE STEPS                         ***
**********************************************************************
**
**                                Step-1
**********************************************************************
*STEP, NAME=step-1, INC=1000
**
*STATIC
 <inc1>,<t1>,1E-8,<inc1>
**
*BOUNDARY, TYPE=DISPLACEMENT
 nright, 1,2, <disp_1>
**
** largest residual,ratio of solution correction,,,alternative residual
** convergence criterion
**
*CONTROLS, PARAMETERS=FIELD, FIELD=DISPLACEMENT
.05,1.0
```

```
*CONTROLS, PARAMETERS=TIME INCREMENTATION
1500,1500,,1500,1500,,,50
*CONTROLS, PARAMETERS=LINE SEARCH
 4,4,0.25,0.25,0.15
**
**
** OUTPUTS
*OUTPUT, FIELD, FREQUENCY=1
*NODE OUTPUT
 U,RF
*ELEMENT OUTPUT
E,S
*OUTPUT, FIELD, FREQ=1
 U,RF
*ELEMENT OUTPUT
E,S
*ELEMENT OUTPUT
1,2,3,4,5,6,7,8,9,10
UVARM, S, E, SSAVG, SE
*ELEMENT OUTPUT
11,12,13,14,15,16,17,18,19,20
UVARM, S, E, SSAVG, SE
*ELEMENT OUTPUT
21,22,23,24,25,26,27,28,29,30
UVARM, S, E, SSAVG, SE

**
*OUTPUT, HISTORY, FREQUENCY=1
*NODE OUTPUT, NSET=nright
 U,RF
**
*Restart, write, frequency=0
**
** FIELD OUTPUT: F-Output-1
**
*Output, field, variable=PRESELECT
**
** HISTORY OUTPUT: H-Output-1
**
*Output, history, variable=PRESELECT
*ENDSTEP
**
**
************************************************************************
***                              END                                 ***
************************************************************************
```

MCID_v3Example.ma file

```
  6
** MAT. #1: MATERIAL NAME: Description of the material
   CAR-EPO-1
** E22,       E11,       nu12 ,      G21,    GIc,    GIIc, YTUD, totalthick
   8900.0, 172000.0,   0.35,   4200.0,  0.765,  1.250,41.43,6.0
** thick,      layers,  SLDAT
   0.250,   11.0,   69.40
** X1co, X2co, X6co, X12co,X16co,X26co
   28655.73, 209.22,   248.22,   -2997246.76,  6533010.64,  -48036.18
** X1cc, X2cc, X6cc, X12cc,X16cc,X26cc
   87444.38, 646.84,   255.66,   -28281175.89,  11177953.00,  -82684.84
** X1phy, X2phy, X6phy, X12phy,X16phy,X26phy
   772.47, 125.81,   247.73,   -59628.89,  -1964070.85,  -56922.25
** MAT. #2: MATERIAL NAME: Description of the material
   CAR-EPO-2
** E22,       E11,       nu12 ,      G21,    GIc,    GIIc, YTUD, totalthick
   8900.0, 172000.0,   0.35,   4200.0,  0.765,  1.250,41.43, 6.0
** thick,      layers,  SLDAT
   0.250,   11.0,   69.40
** X1co, X2co, X6co, X12co,X16co,X26co
   40737.66, 297.43,   353.25,   -6057367.20,  -13271238.65,  97584.23
** X1cc, X2cc, X6cc, X12cc,X16cc,X26cc
   124364.43, 919.94,   363.60,   -57203941.98,  -22609490.39,  167245.48
** X1phy, X2phy, X6phy, X12phy,X16phy,X26phy
   1088.80, 177.87,   352.53,   -118496.29,  3921474.98,  115925.83
** MAT. #3: MATERIAL NAME: Description of the material
   CAR-EPO-3
** E22,       E11,       nu12 ,      G21,    GIc,    GIIc, YTUD, totalthick
   8900.0, 172000.0,   0.35,   4200.0,  0.765,  1.250,41.43,6.0
** thick,      layers,  SLDAT
   0.500,   11.0,   69.40
** X1co, X2co, X6co, X12co,X16co,X26co
   25705.82, 206.67,   244.28,   -2656296.21,  -951917492.01,  7653633.61
** X1cc, X2cc, X6cc, X12cc,X16cc,X26cc
   40879218861431259000.00, 385525281148999680.00,   244.28,   -
6456134217708192500000000000000000000.00,  -3165105232108985500000.00,
16942963769846946000.00
** X1phy, X2phy, X6phy, X12phy,X16phy,X26phy
   1568.03, 172.69,   244.27,   -225905.96,  359430257.34,  8968374.81
** MAT. #4: MATERIAL NAME: Description of the material
   CAR-EPO-4
** E22,       E11,       nu12 ,      G21,    GIc,    GIIc, YTUD
   8900.0, 172000.0,   0.35,   4200.0,  0.765,  1.250,41.43
** thick,      layers,  SLDAT
   0.250,   11.0,   69.40
** X1co, X2co, X6co, X12co,X16co,X26co
   57876.11, 422.56,   502.80,   -12226150.95,  26769314.19,  -196827.97
** X1cc, X2cc, X6cc, X12cc,X16cc,X26cc
   177122.95, 1310.20,   517.85,   -116033474.60,  45861485.05,  -339243.65
** X1phy, X2phy, X6phy, X12phy,X16phy,X26phy
   2029.60, 295.35,   502.21,   -405456.24,  -17460980.72,  -216672.39
** MAT. #5: MATERIAL NAME: Description of the material
   CAR-EPO-5
** E22,       E11,       nu12 ,      G21,    GIc,    GIIc, YTUD, totalthick
   8900.0, 172000.0,   0.35,   4200.0,  0.765,  1.250,41.43, 6.0
** thick,      layers,  SLDAT
   0.250,   11.0,   69.40
** X1co, X2co, X6co, X12co,X16co,X26co
   64812.70, 473.20,   563.28,   -15332375.15,  -33608602.11,  247116.32
** X1cc, X2cc, X6cc, X12cc,X16cc,X26cc
   198412.73, 1467.69,   580.09,   -145603792.28,  -57548963.05,  425697.51
** X1phy, X2phy, X6phy, X12phy,X16phy,X26phy
   2310.72, 333.51,   562.65,   -524896.41,  23218599.71,  271112.07
** MAT. #6: MATERIAL NAME: Description of the material
   CAR-EPO-6
** E22,       E11,       nu12 ,      G21,    GIc,    GIIc, YTUD, totalthick
   8900.0, 172000.0,   0.35,   4200.0,  0.765,  1.250,41.43, 6.0
** thick,      layers,  SLDAT
```

```
       1.000,   11.0,   69.40
    ** X1co, X2co, X6co, X12co,X16co,X26co
       25682.08, 206.48,   244.02,   -2651394.07,  -1432372582239897100000.00,
9358306657135462400.00
    ** X1cc, X2cc, X6cc, X12cc,X16cc,X26cc
       41088714792348492000.00, 385691781220892740.00,   244.02,   -
64745791310234351000000000000000000000.00,  -3193131147300964400000.00,
16955897519920749000.00
    ** X1phy, X2phy, X6phy, X12phy,X16phy,X26phy
       1939.59, 182.28,   244.02,   -330341.50,  391529118758253360000.00,
11043309641135532000.00
```

Example III: Results of ply 3 of the model in section 7.2.

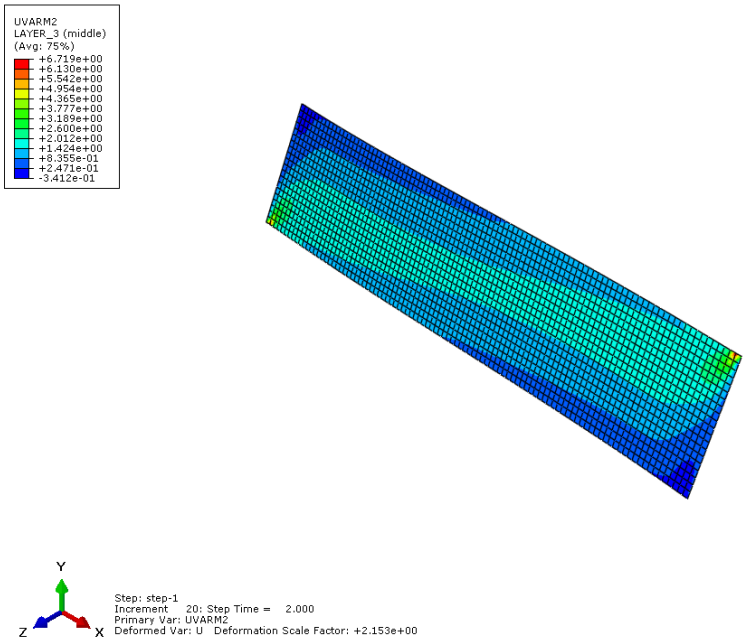

Figure 4 UVARM1 variable results for ply 3 in Substep 20

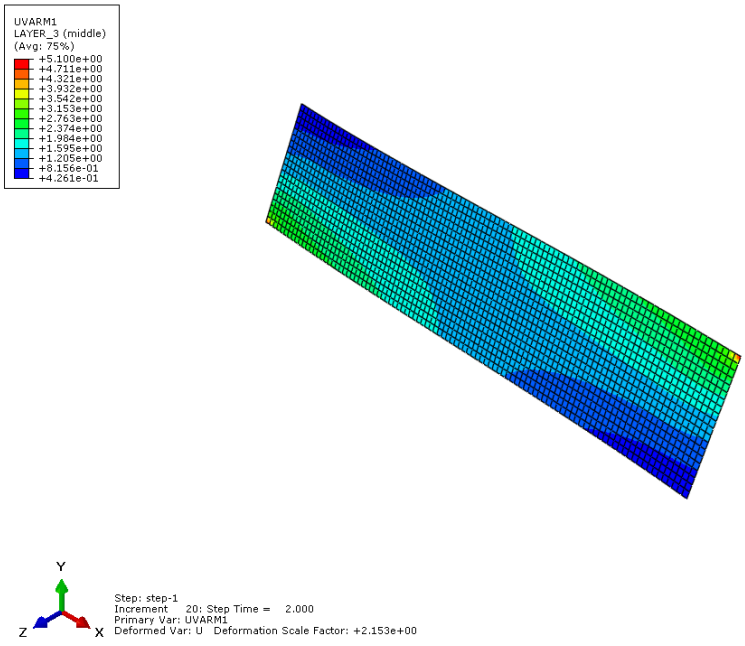

Figure 5 UVARM2 variable results for ply 3 in Substep 20

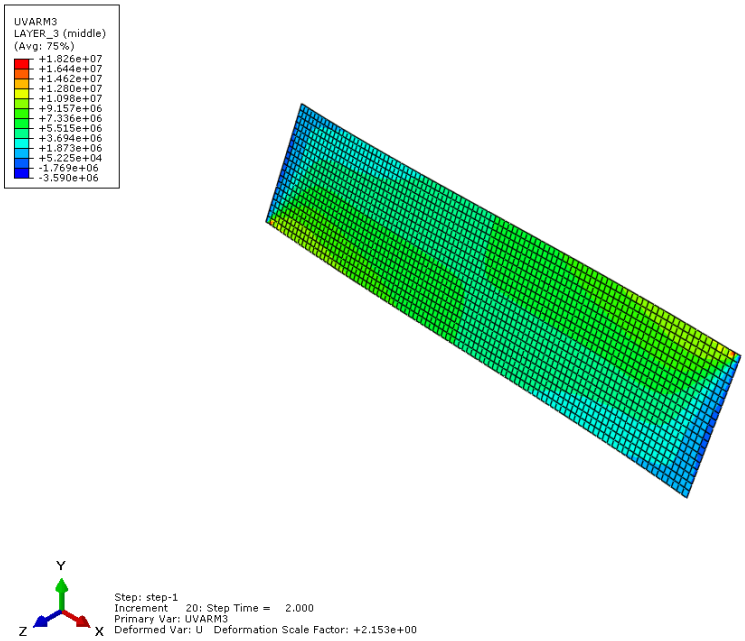

Figure 6 UVARM3 variable results for ply 3 in Substep 20

References

[1] Camanho, P.P., Dávila, C.G., Pinho, S.T., Iannucci, L. and Robinson, P., 2006. Prediction of in situ strengths and matrix cracking in composites under transverse tension and in-plane shear. *Composites Part A: Applied Science and Manufacturing*, 37(2), pp. 165-176.

[2] L.Zubillaga, A.Turon., P.Maimi, J.Costa, S.Mahdi and P.Linde. 2014. An energy based failure criterion for matrix crack induced delamination in laminated composite structures. *Composite Structures*. 114, pp 339-341

[3] Maimí, P., Camanho, P.P., Mayugo, J.A. and Turon, A. 2011. Matrix cracking and delamination in laminated composites: Part I: Ply consitutive law, first ply failure and onset of delamination. *Mechanics of materials*. 43, pp. 169-185.

[4] O'Brien, T.K., 1985. Analysis of local delaminations and their influence on composite laminate behavior. 1985,*ASTM Special Technical Publication* , pp. 282-297.